Mathematical models of the human eye

Rodolfo Repetto

Department of Civil, Chemical and Environmental Engineering
University of Genoa, Italy
Email: rodolfo.repetto@unige.it
Phone: +39 010 3532471
http://dicca.unige.it/rrepetto/
skype contact: rodolfo-repetto

May 2016

Table of contents I

Table of contents II

Table of contents III

Acknowledgements

The present notes have been prepared in collaboration with **Jennifer H. Tweedy** (Department of Bioengineering, Imperial College London, UK). Mariia Dvoriashyna provided the plots for the flow in the posterior chamber.

Introduction to the fluid mechanics of the human eye

Introduction to biofluid dynamics

What is biological fluid mechanics?

Biological fluid mechanics (or *biofluid mechanics*) is the study of the motion of biological fluids in any possible context (e.g. blood flow in arteries, animal flight, fish swimming, ...)

In the present course we will focus on fluid motion in the human eye.

What is biological fluid mechanics useful for?

- **Pure physiology:** understanding how animals, and in particular humans, work.
- **Pathophysiology:** understanding why they might go wrong. In other words understanding the origins and development of diseases.
- **Diagnosis:** recognising diseases from possibly non-traumatic measurements.
- **Cure:** providing support to surgery and to the design of prosthetic devices.

Peculiarities of physiological fluid flows

Thomas Young (1808):

The mechanical motions, which take place in animal body, are regulated by the same general laws as the motion of inanimate bodies . . . and it is obvious that the enquiry, in what matter and in what degree, the circulation of the blood depends on the muscular and elastic powers of the heart and of the arteries, . . . , must become simply a question belonging to the most refined departments of the theory of hydraulics.

There are some key features which characterise physiological flows.

- **Pulsatility.** In most cases physiological flows are highly unsteady and are often pulsatile (e.g. flow in the systemic arteries or in the respiratory system . . .).
- **Complex geometries.** Typically physiological flows take place in very complex geometries. In order to study the problems by analytical means it is therefore necessary to idealise the geometry in a suitable manner. It is a research challenge of recent years to perform numerical simulations on real geometries.
- **Deformability.** Not only the geometry of the flow domain might be complex but it also often varies in time. This typically induces great complication in the mathematical analysis. Often the problem to be solved is effectively a solid-fluid interaction.
- **Low Reynolds number flows.** In many cases of physiological interest (but by no means always) the Reynolds number of the flow is fairly low and this allows simplifying the equations.

Anatomy of the eye

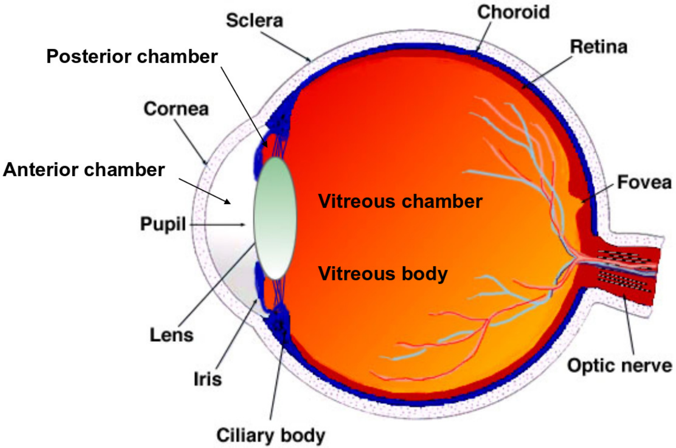

The anterior and posterior chambers

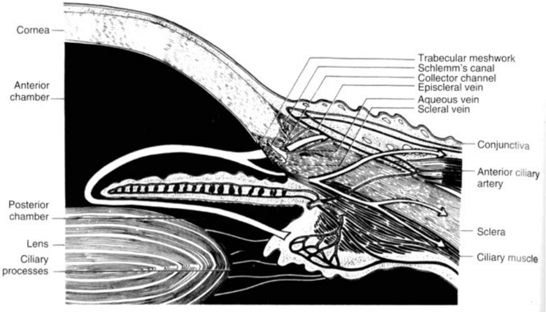

The **anterior chamber** contains the **aqueous humour**, a fluid with approximately the same mechanical characteristics as water

Aqueous humour is produced by the ciliary processes, flows in the **posterior chamber**, through the pupil, in the anterior chamber and is drained out at through the trabecular meshwork and the Schlemm's canal into the venous system.

The aqueous flow has two main roles

- It provides with nutrients the cornea and the lens which are avascular tissues.
- A balance between aqueous production and drainage resistance regulates the intraocular pressure (IOP).

The anterior chamber: drainage system

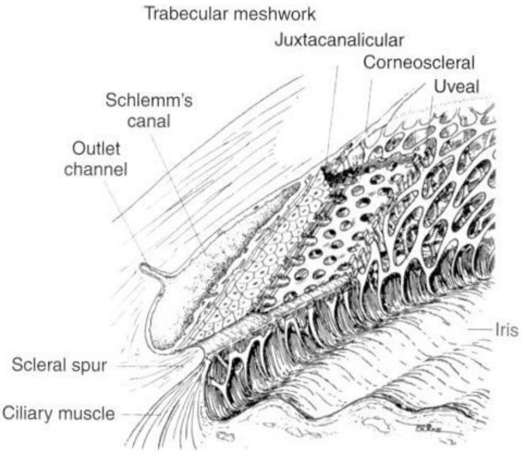

The lens

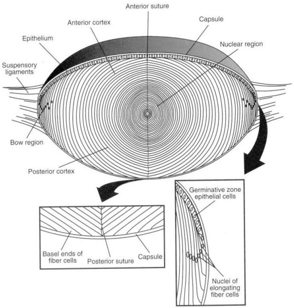

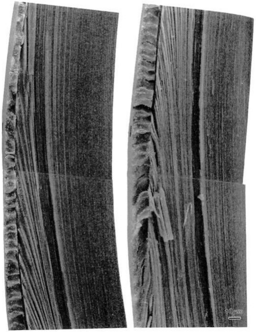

The **lens** is a transparent, biconvex structure in the eye that, along with the cornea, has the role of refracting light rays and to allow focus on the retina. It is responsible for approximately 1/3 of the total eye refractive power. The lens changes the focal distance by changing its shape (**accommodation**).

Structure: The lens is composed by three layers.

- **The capsule** is a smooth, transparent basement membrane that completely surrounds the lens. It is mainly composed of collagen and it is very elastic. Its thickness ranges within 2-28 μm.
- **The lens epithelium** is located in the anterior portion of the lens, between the lens capsule and the lens fibres.
- **The lens fibres** form the bulk of the lens. They are long, thin, transparent and firmly packed to each other. They form an onion-like structure.

The lens accommodation

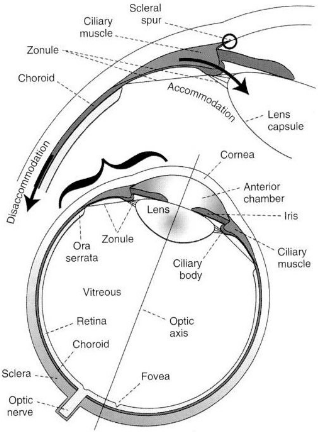

The vitreous chamber

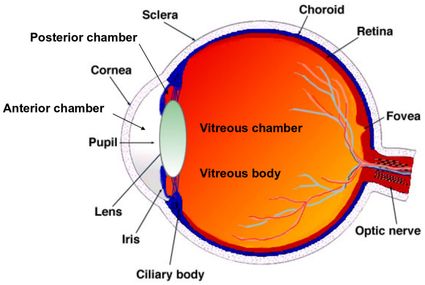

The **vitreous chamber** contains the **vitreous humour**. The vitreous has the following functions:

- **supporting the retina** in contact with the pigment epithelium;
- **filling-up the vitreous cavity**;
- acting as a **diffusion barrier** between the anterior and posterior segments of the eye
- establishing an unhindered path of light from the lens to the retina.

The vitreous goes through considerable physiological changes during life

- disintegration of the gel structure, liquefaction **(synchysis)**;
- approximately linear increase in the volume of liquid vitreous with age;
- possible complete liquefaction;
- **posterior vitreous detachment (PVD)** [film].

Vitreous replacement: After surgery **(vitrectomy)** the vitreous may be completely replaced with tamponade fluids (e.g. silicon oils, aqueous humour, air, . . .).

Optic nerve

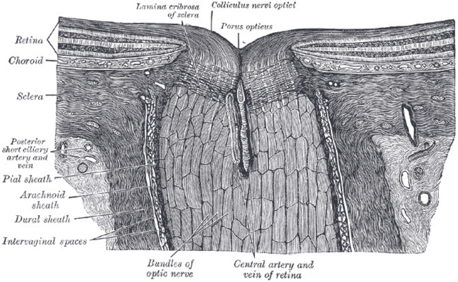
Lamina cribrosa of sclera
Colliculus nervi optici
Porus opticus
Retina
Choroid
Sclera
Posterior short ciliary artery and vein
Pial sheath
Arachnoid sheath
Dural sheath
Intervaginal spaces
Bundles of optic nerve
Central artery and vein of retina

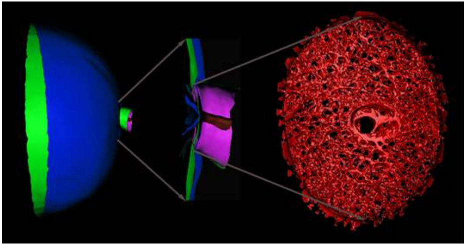

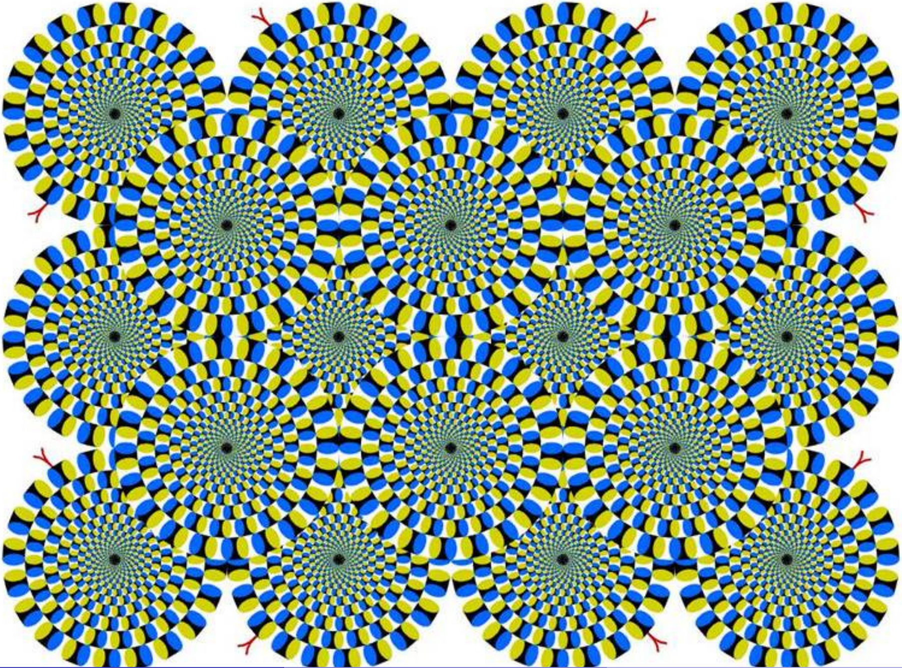

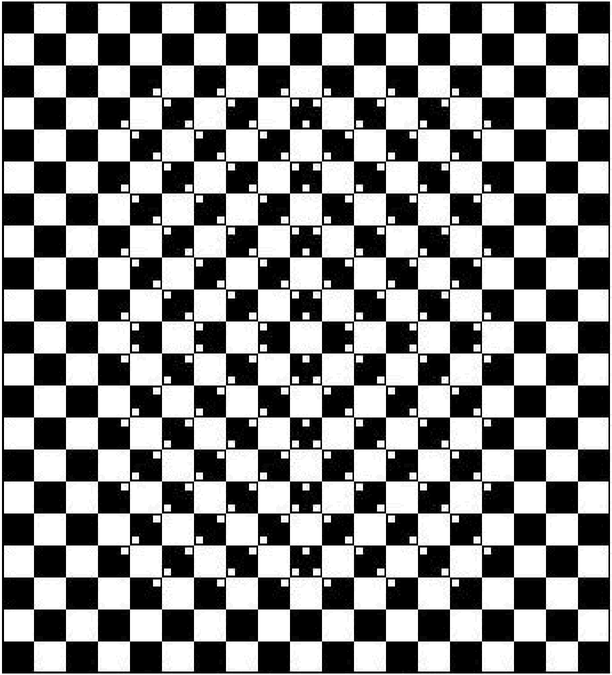

Specific references

- The textbook by Ethier and Simmons (2007) has a section on eye biomechanics.
- Ethier et al. (2004) review biomechanics and biotransport processes in the eye.
- Siggers and Ethier (2012) and Braun (2012) review the fluid mechanics of the eye.

Basic notions of fluid mechanics

The Continuum Approach

Fluids (liquids, gases, ...) are composed of particles (molecules). Each molecule is composed of a central nucleus surrounded by a cloud of electrons. Some typical dimensions are given in the following table

Diameter of	
an atomic nucleus	$2 \cdot 10^{-15}$ m
a gas molecule	$6 \cdot 10^{-10}$ m
Spacing of gas molecules	$3 \cdot 10^{-9}$ m
Diameter of	
a red blood cell	$8 \cdot 10^{-6}$ m
a capillary	$4 - 10 \cdot 10^{-6}$ m
an artery	$\approx 10^{-2}$ m

In most applications of fluid mechanics, the typical spatial scale under consideration, L, is much larger than the spacing between molecules, l. In this case we suppose the material to be composed of elements whose size is small compared to L but large compared to l. We then assume each fluid element occupies a point in space.

We assume each property, F, of the fluid (e.g. density, pressure, velocity, ...), to be a continuous function of space $\mathbf{x}$ and time t

$$F = F(\mathbf{x}, t).$$

Forces on a continuum I

Two kind of forces can act on a continuum body

- **body forces;**
- **surface forces.**

Body forces

These forces are slowly varying in space. If we consider a small volume, δV, the force is approximately constant over it. Therefore the force on the volume is

$$\delta \mathbf{F} = \tilde{\mathbf{f}} \delta V,$$

where $\mathbf{f}$ is the force per unit volume. In most cases of interest for this course $\delta \mathbf{F}$ is proportional to the mass of the element. Therefore we may write

$$\delta \mathbf{F} = \rho \mathbf{f} \delta V,$$

where ρ denotes the fluid density, i.e. mass per unit volume ($[\rho] = ML^{-3}$), and $\mathbf{f}(\mathbf{x}, t)$ is independent of the density.

The vector field $\mathbf{f}$ is termed the **body force field**, and has the dimensions of acceleration or force per unit mass

$$[\mathbf{f}] = LT^{-2}.$$

In general $\mathbf{f}$ and $\tilde{\mathbf{f}}$ depend on space and time: $\mathbf{f} = \mathbf{f}(\mathbf{x}, t)$ and $\tilde{\mathbf{f}} = \tilde{\mathbf{f}}(\mathbf{x}, t)$. If we want to compute the total force $\mathbf{F}$ on a finite volume V we need to integrate $\mathbf{f}$ over V

$$\mathbf{F} = \iiint_V \tilde{\mathbf{f}} dV = \iiint_V \rho \mathbf{f} dV.$$

Forces on a continuum II

Surface forces

The force is approximately constant over a small surface δS, and therefore the force on the surface is

$$\delta \mathbf{\Sigma} = \mathbf{t} \delta S,$$

where $\mathbf{t}$ is the force per unit area or **tension**, and has dimensions given by

$$[\mathbf{t}] = ML^{-1}T^{-2}.$$

As well as depending on position $\mathbf{x}$ and time t, the vector $\mathbf{t}$ also depends on the orientation of the surface. The orientation is uniquely specified by the unit vector $\mathbf{n}$ normal to the surface, meaning that $\mathbf{t} = \mathbf{t}(\mathbf{x}, t, \mathbf{n})$.

To compute the force $\mathbf{\Sigma}$ on a surface S we must integrate

$$\mathbf{\Sigma} = \iint_S \mathbf{t} dS.$$

Cauchy's principle and the stress tensor

Cauchy's stress principle asserts that

"When a continuum body is acted on by forces, i.e. surface forces and body forces, there are internal reactions throughout the body acting between the material points."

Based on this principle, Cauchy demonstrated that the state of stress at a point in a continuum body is completely defined by the nine components σ_{ij} of a **second-order tensor** called the **Cauchy stress tensor**.

The stress vector $\mathbf{t}(\mathbf{n})$ at any point P, acting on a plane of normal vector $\mathbf{n}$, can be expressed in terms of the stress tensor

$$\text{in component form as} \quad t_i(\mathbf{n}) = \sigma_{ij} n_j, \quad \text{or in vector form as} \quad \mathbf{t}(\mathbf{n}) = \boldsymbol{\sigma} \cdot \mathbf{n},$$

where σ_{ij} represents the ith component of the stress on the plane with normal $\mathbf{e}_j$.

Properties of the stress tensor

- **The stress tensor is symmetric**, i.e. $\sigma_{ij} = \sigma_{ji}$.
- The terms on the principal diagonal of the stress tensor matrix are termed the **normal stresses**. The other six (not on the principal diagonal) are **shear stresses.**
- In a fluid at rest we have

  $$\text{in component form as} \quad \sigma_{ij} = -p\delta_{ij}, \quad \text{or in vector form as} \quad \boldsymbol{\sigma}(\mathbf{n}) = -p\mathbf{I},$$

  where $p(\mathbf{x}, t)$ is the **pressure** and δ_{ij} is the Kronecker delta. In this case the stress tensor is **a multiple of the identity.**

Statics of fluids I

Equation of statics in integral form

Given a volume V with surface S, the equilibrium of forces acting on the body can be written as

$$\iiint_V \rho \mathbf{f} \, dV + \iint_S \mathbf{t} \, dS = 0.$$

For a fluid at rest, since $\mathbf{t} = -p\mathbf{n}$, we can write

$$\iiint_V \rho \mathbf{f} \, dV + \iint_S -p\mathbf{n} \, dS = 0, \tag{1}$$

and applying Gauss' theorem

$$\iiint_V (\rho \mathbf{f} - \boldsymbol{\nabla} p) \, dV = 0.$$

It can be shown that there are no resultant moments acting on the volume, and therefore equation (1) provides necessary and sufficient conditions for equilibrium.

Equation of statics in differential form

Since the volume V is arbitrary, the integrand must be zero everywhere

$$\rho \mathbf{f} - \boldsymbol{\nabla} p = 0. \tag{2}$$

Statics of fluids II

Incompressible fluids in a gravitational field

For many problems of practical relevance we can assume

- $\rho =$constant;
- $\mathbf{f} = (0, 0, -g)$, with respect to a system of coordinates (x_1, x_2, x_3) with x_1 and x_2 horizontal and x_3 pointing vertically upward, and with g being the acceleration of gravity ($g \approx 9.81$ m s^{-2}).

In this case equation (2) can be easily solved, leading to the following result, known as **Stevin's law**

$$h = x_3 + \frac{p}{\gamma} = \text{const.},$$

where $\gamma = \rho g$ is the specific weight (force per unit volume) of the fluid ($[\gamma] = ML^{-2}T^{-2}$).

This implies that the **pressure increases linearly as we move vertically downwards, and the rate of increase is equal to the specific weight of the fluid**.

Basic notions of kinematics of fluids I

Kinematics is the study of fluid motion.
Two main approaches are adopted in fluid mechanics

- **Eulerian reference frame (spatial approach);**
- **Lagrangian reference frame (material approach).**

Eulerian or spatial approach

We define a system of coordinates fixed in space, $\mathbf{x} = (x_1, x_2, x_3)$. This means that any vector $\mathbf{x}$ denotes a particular point in space (note that this point will, in general, be occupied by different fluid particles at different times).

When a fluid property (say F) is described as $F_S(\mathbf{x}, t)$, it tells us how F varies in time at a fixed point in space. We can also define $\partial F_S(\mathbf{x}, t)/\partial t$, which is the rate of change in time of F in $\mathbf{x}$. In most cases this approach is very convenient.

Important note on derivatives:
Consider the velocity field, i.e. we take $F = \mathbf{u}$. If we take the partial derivative of $\mathbf{u}$ with respect to time, i.e. $\partial \mathbf{u}(\mathbf{x}, t)/\partial t$, we **do not get the acceleration of the fluid!** This is because the point $\mathbf{x}$ is, in general, occupied by different fluid particles at different times. The quantity $\partial \mathbf{u}(\mathbf{x}, t)/\partial t$ is the rate of change of the velocity at a single point rather than the rate of change of the velocity of fluid particles (which we usually term the acceleration). We will return to this point shortly.

Basic notions of kinematics of fluids II

Lagrangian or material approach

We define $\mathbf{X} = (X_1, X_2, X_3)$ as a system of coordinates fixed with material particles. This means that any value of $\mathbf{X}$ is always associated with a particular fluid particle.

Any fluid property F can then be described as $F_M(\mathbf{X}, t)$. This tells us how the value of F associated with a material fluid particle varies in time. We can define $\partial F_M(\mathbf{X}, t)/\partial t$, which is the rate of change in time of F associated with the particle $\mathbf{X}$.

As the meaning of this time derivative is different from that taken with the Eulerian approach, different notations are often adopted

$$\frac{\partial F_S(\mathbf{x}, t)}{\partial t} = \frac{\partial F}{\partial t},$$
$$\frac{\partial F_M(\mathbf{X}, t)}{\partial t} = \frac{DF}{Dt}.$$

In some cases the Lagrangian approach is more convenient (e.g. it is often used for studying fluid mixing).

Important note on derivatives:
In this case the partial derivative of $\mathbf{u}$ with respect to t does give the acceleration $\mathbf{a}$

$$\frac{\partial \mathbf{u}(\mathbf{X}, t)}{\partial t} = \frac{D\mathbf{u}}{Dt} = \mathbf{a}.$$

Basic notions of kinematics of fluids III

Material derivative with respect to spatial coordinates

We can establish a relationship between the Eulerian and Lagrangian approaches if we know the function

$$\mathbf{x} = \mathbf{x}(\mathbf{X}, t), \tag{3}$$

which is well defined since a point in space cannot be occupied by two particles. The above equation represents the position $\mathbf{x}$ of a material particle, identified by $\mathbf{X}$, in time. This is called **particle trajectory**.

Since a particle cannot occupy two different points in space, equation (3) is invertible. Therefore we can write

$$\mathbf{X} = \mathbf{X}(\mathbf{x}, t).$$

Using (3) we can write

$$F_S(\mathbf{x}, t) = F_S[\mathbf{x}(\mathbf{X}, t)] = F_M(\mathbf{X}, t).$$

Let us now consider a material derivative of any fluid property F

$$\frac{DF}{Dt} = \left.\frac{\partial F_M(\mathbf{X}, t)}{\partial t}\right|_{\mathbf{X}} = \left.\frac{\partial F_S(\mathbf{x}(\mathbf{X}, t), t)}{\partial t}\right|_{\mathbf{X}} = \left(\frac{\partial F_S}{\partial t}\right)_{\mathbf{x}} + \left(\frac{\partial F_S}{\partial x_i}\right)_t \left(\frac{\partial x_i}{\partial t}\right)_{\mathbf{X}} = \frac{\partial F_S}{\partial t} + u_i \frac{\partial F_S}{\partial x_i}. \tag{4}$$

We can use this formula to compute the material derivative of F at each point in space and time.

Basic notions of kinematics of fluids IV

In particular, we can define the particle acceleration in terms of spatial coordinates as

$$\mathbf{a} = \frac{D\mathbf{u}}{\partial t} = \frac{\partial \mathbf{u}}{\partial t} + (\mathbf{u} \cdot \boldsymbol{\nabla})\mathbf{u} \quad \text{or} \quad a_i = \frac{\partial u_i}{\partial t} + u_j \frac{\partial u_i}{\partial x_j}.$$

Basic notions of kinematics of fluids V

Flow field

- **Steady flow**
  If the spatial velocity does not depend on time in the Eulerian reference frame, the flow field is said to be steady
  $$\mathbf{u} = \mathbf{u}(\mathbf{x}).$$
- **Uniform flow**
  If the spatial velocity does not depend on space the flow is said to be uniform
  $$\mathbf{u} = \mathbf{u}(t).$$
- **Streamlines**
  We define a streamline as a line which is everywhere tangent to the velocity vectors. Streamlines are defined by the solution of the equation
  $$d\mathbf{x} \times \mathbf{u}(\mathbf{x}, t) = 0,$$
  at a fixed time t. Alternatively
  $$\frac{dx_1}{u_1} = \frac{dx_2}{u_2} = \frac{dx_3}{u_3}.$$
  In steady flows streamlines and particle trajectories are coincident.

Principle of conservation of mass

"The mass of a material body[1] within a continuum remains constant in time."

The above principle can be expressed mathematically in differential form as

$$\frac{\partial \rho}{\partial t} + \nabla \cdot (\rho \mathbf{u}) = 0. \tag{5}$$

Incompressible fluids

An **incompressible fluid** is one whose density $\rho(\mathbf{x}, t)$ is constant.

- **To a good approximation, many liquids are incompressible.**
- **The assumption of incompressibility is good for most internal fluid flows in mathematical biology.**

For an incompressible fluid, the principle of mass conservation is equivalent to

$$\nabla \cdot \mathbf{u} = 0. \tag{6}$$

[1] A material body is a body that is always composed of the same fluid particles.

Principle of conservation of momentum

"The time derivative of the momentum of a material body of continuum equals the resultant of all the external forces acting on it."

In differential form this can be expressed as

$$\rho \left(\frac{\partial}{\partial t} \mathbf{u} + (\mathbf{u} \cdot \nabla \mathbf{u}) - \mathbf{f} \right) = \nabla \cdot \boldsymbol{\sigma}, \tag{7}$$

where $\boldsymbol{\sigma}$ is the stress tensor.

"The time derivative of the angular momentum of a material body of continuum equals the resultant of all external moments acting on it."

Using this principle it can be shown that the stress tensor $\boldsymbol{\sigma}$ is symmetric.

Definition of pressure in a moving fluid I

We have seen that, **in a fluid at rest,** the stress tensor takes the simple form

$$\sigma_{ij} = -p\delta_{ij},$$

where the scalar p is the static pressure.
In the case of a moving fluid, the situation is more complicated. In particular:

- the tangential stresses are not necessarily equal to zero;
- the normal stresses can depend on the orientation of the surface they act on.

Therefore the notion that the normal stress is the pressure, which acts equally in all directions is lost. We can define the pressure in a moving fluid as

$$p = -\frac{1}{3}\sigma_{ii}, \qquad \text{or,} \qquad p = -\frac{1}{3}\,\mathrm{tr}(\boldsymbol{\sigma}).$$

Important note

- **Compressible fluids**
  From classical thermodynamics it is known that we can define the pressure of the fluid as a **parameter of state**, making use of an **equation of state**. Thermodynamical relations refer to equilibrium conditions, so we can denote the thermodynamic pressure as p_e.
- **Incompressible fluids**
  For an incompressible fluid the pressure p is an independent, purely dynamical, variable.

Definition of pressure in a moving fluid II

In the following we will consider **incompressible fluids** only.
It is usually convenient to split to the stress tensor σ_{ij} into an **isotropic part**, $-p\delta_{ij}$, and a **deviatoric part**, d_{ij}, which is entirely due to fluid motion. Thus we write

$$\sigma_{ij} = -p\delta_{ij} + d_{ij}.$$

The tensor d_{ij} accounts for tangential stresses and also normal stresses, whose components sum to zero.

Constitutive relationship for Newtonian fluids I

A **constitutive law** links the stress tensor to the kinematic state of the fluid.

- **This law provides a third relationship, which, together with the equations of mass and momentum conservation, closes the problem for the velocity and pressure fields.**

The constitutive law for **Newtonian fluids** can be obtained by assuming the following:

1. The deviatoric part of the stress tensor, $\mathbf{d}$, is a continuous function of the **rate-of-strain** tensor $\mathbf{e}$, defined as

$$\text{in component form,} \quad e_{ij} = \frac{1}{2}\left(\frac{\partial u_i}{\partial x_j} + \frac{\partial u_j}{\partial x_i}\right) \quad \text{or, in vector form,} \quad \mathbf{e} = \frac{1}{2}\left(\nabla \mathbf{u} + (\nabla \mathbf{u})^T\right).$$

2. If $\mathbf{e} = \mathbf{0}$ (i.e. the flow is **uniform**) then $\mathbf{d} = \mathbf{0}$. This means that $\boldsymbol{\sigma} = -p\mathbf{I}$, i.e. the stress reduces to the stress in static conditions.
3. The fluid is homogeneous, i.e. $\boldsymbol{\sigma}$ does not depend explicitly on $\mathbf{x}$.
4. The fluid is isotropic, i.e. there is no preferred direction.
5. The relationship between $\mathbf{d}$ and $\mathbf{e}$ is linear.
6. The fluid is incompressible.

These assumptions imply that

$$\text{in component form,} \quad \sigma_{ij} = -p\delta_{ij} + 2\mu e_{ij}, \quad \text{or, in vector form,} \quad \boldsymbol{\sigma} = -p\mathbf{I} + 2\mu\mathbf{e}, \qquad (8)$$

where μ is the **dynamic viscosity**.

Constitutive relationship for Newtonian fluids II

Definitions

- The **dynamic viscosity** μ has dimensions $[\mu] = ML^{-1}T^{-1}$.
- It is often convenient to define the **kinematic viscosity** as

$$\nu = \frac{\mu}{\rho}.$$

The kinematic viscosity has dimensions $[\nu] = L^2T^{-1}$.

Inviscid fluids

A fluid is said to be **inviscid** or **ideal** if $\mu = 0$. For an inviscid fluid the constitutive law (8) becomes

$$\text{in component form,} \quad \sigma_{ij} = -p\delta_{ij}, \quad \text{or, in vector form,} \quad \boldsymbol{\sigma} = -p\mathbf{I}. \tag{9}$$

Thus the motion of the fluid does not affect the stress. Note that there are no truly inviscid fluids in nature. However, the inviscid approximation is good in certain cases, such as fast flows of a low-viscosity fluid.

The Navier-Stokes equations

Substituting the constitutive law (8) into the equation for conservation of motion (7), we obtain

$$\frac{\partial u_i}{\partial t}+u_j\frac{\partial u_i}{\partial x_j}-f_i+\frac{1}{\rho}\frac{\partial p}{\partial x_i}-\nu\frac{\partial^2 u_i}{\partial x_j \partial x_j}=0, \quad \text{or, in vector form,} \quad \frac{\partial \mathbf{u}}{\partial t}+(\mathbf{u}\cdot\nabla)\mathbf{u}-\mathbf{f}+\frac{1}{\rho}\nabla p-\nu\nabla^2\mathbf{u}=0, \tag{10}$$

where $\mathbf{f} = f_i\mathbf{e}_i$ is the resultant external body force acting on the fluid. Recalling the definition of material derivative (4) the above equation can also be written as

$$\frac{Du_i}{Dt}-f_i+\frac{1}{\rho}\frac{\partial p}{\partial x_i}-\nu\frac{\partial^2 u_i}{\partial x_j^2}=0, \quad \text{or, in vector form,} \quad \frac{D\mathbf{u}}{Dt}-\mathbf{f}+\frac{1}{\rho}\nabla p-\nu\nabla^2\mathbf{u}=0.$$

This equation is called the **Navier-Stokes equation**, and it is of fundamental importance in fluid mechanics. It is actually three equations, one for each spatial component. The equations govern the motion of a Newtonian incompressible fluid and should to be solved together with the continuity equation (6).

Buckingham's Π theorem I

In fluid dynamics problems one often wishes to find a physical quantity in terms of other variables in the problem, that is

$$a = f(a_1, \dots, a_k),$$

where a is the quantity of interest and a_i $(i = 1, 2, \dots, k)$ are other variables and parameters in the problem.
The Buckingham Π theorem states that equation (38) is equivalent to

$$\Pi = \mathcal{F}(\Pi_1, \dots, \Pi_m),$$

where $m \leq k$ and the quantities Π, Π_1, Π_2, ..., Π_m are all dimensionless. The number of variables that have been removed, $k - m$, equals the number of **independent dimensions** in the variables a_i.

- In fluid dynamics problems, we often have $k - m = 3$, since all variables have dimensions that are combinations of **length, time and mass**, leading to three independent dimensions.
- **Rescaling** or **nondimensionalising** is a powerful tool in fluid mechanics, as, through simplifying a problem, it enables us to obtain a great deal of insight.

Dimensionless Navier-Stokes equations I

When dealing with theoretical modelling of physical phenomena, it is convenient to work with dimensionless equations. The main reasons are:

- the number of parameters in the problem decreases if one passes from a dimensional to a dimensionless formulation;
- if proper scalings are adopted, it is much easier to evaluate the relative importance of different terms appearing in one equation.

Let us consider the Navier-Stokes equation and assume that the body force is gravity. Equations (10) can then be written as

$$\underbrace{\frac{\partial \mathbf{u}}{\partial t} + (\mathbf{u}\cdot\nabla)\mathbf{u}}_{①} = \underbrace{\mathbf{g}}_{②} \underbrace{-\frac{1}{\rho}\nabla p}_{③} + \underbrace{\nu\nabla^2\mathbf{u}}_{④} = 0, \tag{11}$$

where the vector $\mathbf{g}$, representing the gravitational field, has magnitude g and is directed vertically downwards. We recall the physical meaning of all terms:

- ①: convective terms;
- ②: gravity;
- ③: pressure gradient;
- ④: viscous term.

Dimensionless Navier-Stokes equations II

We will now scale the Navier–Stokes equation. Suppose that L is a characteristic length scale of the domain under consideration and U a characteristic velocity. We can introduce the following dimensionless coordinates and variables

$$\mathbf{x}^* = \frac{\mathbf{x}}{L}, \qquad \mathbf{u}^* = \frac{\mathbf{u}}{U}, \qquad t^* = \frac{t}{L/U},$$

where superscript stars indicate dimensionless quantities.
In scaling the pressure there are two commonly used possibilities:

1. The pressure gradient, ③, balances with the viscous forces, ④, leading to

$$p^* = \frac{p}{\rho\nu U/L}.$$

   This is the most relevant case for studying physiological flows, for reasons that will be made clear in the following.

2. The pressure gradient, ③, balances with the convective terms, ①, giving

$$p^* = \frac{p}{\rho U^2}.$$

Dimensionless Navier-Stokes equations III

Low-Reynolds-number flows

Let us consider the first case $p = (\mu U/L)p^*$. Equation (11) becomes

$$Re\left[\frac{\partial \mathbf{u}^*}{\partial t^*} + (\mathbf{u}^* \cdot \nabla^*)\mathbf{u}^*\right] + \frac{Re}{Fr^2}\hat{\mathbf{z}} + \nabla^* p^* - \nabla^{*2}\mathbf{u}^* = 0, \qquad (12)$$

where $\hat{\mathbf{z}}$ is the upward directed vertical unit vector.
In the above equation we have introduced two dimensionless parameters.

- $Re = \dfrac{UL}{\nu}$: **Reynolds number**. This represents the ratio between the magnitude of inertial (convective) terms and viscous terms. It plays a fundamental role in fluid mechanics.
- $Fr = \dfrac{U}{\sqrt{gL}}$: **Froude number**. This represents the square root of the ratio between the magnitude of inertial (convective) terms and gravitational terms. It plays a fundamental role when gravity is important, e.g. in free surface flows.

If we now consider the limit $Re \to 0$ the dimensionless Navier-Stokes equation (12) reduces to the so called **Stokes equation**, i.e.

$$\nabla^* p^* - \nabla^{*2}\mathbf{u}^* = 0.$$

This equation is much simpler to solve than the Navier-Stokes equation, primarily because it is linear.

Dimensionless Navier-Stokes equations IV

High-Reynolds-number flows

We now consider the case in which the pressure gradient balances the convective terms. The dimensionless Navier-Stokes equation takes the form

$$\frac{\partial \mathbf{u}^*}{\partial t^*} + (\mathbf{u}^* \cdot \nabla^*)\mathbf{u}^* + \frac{1}{Fr^2}\mathbf{z} + \nabla^* p^* - \frac{1}{Re}\nabla^{*2}\mathbf{u}^* = 0. \tag{13}$$

In the limit $Re \to \infty$ the viscous term in equation (13) tends to zero. Thus at large values of Re the fluid behaves as an **ideal** or **inviscid fluid**.

However, this limit leads to a qualitative change in the Navier–Stokes equation (13). The viscous term contains the highest order derivatives in equation (13), and therefore, if it is neglected, it is not possible to impose the usual number of boundary conditions. To resolve this, we assume that thin **boundary layers** form at the boundaries, and within these the viscous terms in the Navier-Stokes equations have the same magnitude as the convective terms.

If we are only interested in the flow away from the boundaries, we may compute this by solving equation (13) in the limit $Re \to \infty$ and applying no-penetration boundary conditions (no fluid flow through the boundary, rather than the full no-slip conditions).

The dynamic pressure

We now assume that the body force acting on the fluid is gravity, therefore we set in the Navier-Stokes equation (10) $\mathbf{f} = \mathbf{g}$. When ρ is constant the pressure p in a point $\mathbf{x}$ of the fluid can be written as

$$p = p_0 + \rho \mathbf{g} \cdot \mathbf{x} + P, \tag{14}$$

where p_0 is a constant and $p_0 + \rho \mathbf{g} \cdot \mathbf{x}$ is the pressure that would exist in the fluid if it was at rest. Finally, P is the part of the pressure which is associated to fluid motion and can be named **dynamic pressure**. This is in fact the departure of pressure from the hydrostatic distribution.
Therefore, in the Navier-Stokes equations, the term $\rho \mathbf{g} - \nabla p$ can be replaced with $-\nabla P$.
Thus we have:

$$\begin{aligned} &\nabla \cdot \mathbf{u} = 0, \\ &\frac{\partial \mathbf{u}}{\partial t} + (\mathbf{u} \cdot \nabla)\mathbf{u} + \frac{1}{\rho} \nabla P - \nu \nabla^2 \mathbf{u} = 0. \end{aligned} \tag{15}$$

If the Navier-Stokes equations are written in terms of the dynamic pressure gravity does not explicitly appear in the equations.
In the following whenever gravity will not be included in the Navier-Stokes this will be done with the understanding that the pressure is the dynamic pressure (even if p will sometimes be used instead of P).

Lubrication theory I

This technique provides a good approximation to the real solution as long as **the domain of the fluid is long and thin**. It is used because it results in a **considerable simplification** of the Navier–Stokes equations. An example where lubrication theory has been successfully used to analyse a problem is in blood flow in a capillary, specifically in the small gap between a red blood cell and the wall of the capillary.

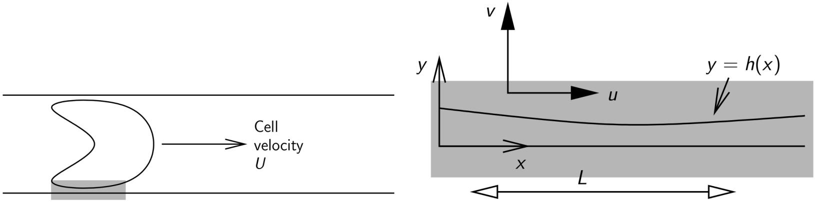

Example of a scenario where lubrication theory may be applied. A cell moves steadily with speed U along a vessel with a narrow gap at the walls (Secomb, 2003).

Lubrication theory applies if one dimension of the space occupied by the fluid is much smaller than the other(s).

Lubrication theory II

Mathematical formulation

For simplicity let us assume that the flow is two dimensional (all derivatives with respect to the third coordinate, say z, may be neglected) and that the height of the domain is $h(x)$ and a typical streamwise length is L.

The fluid velocity at the vessel walls is zero (no-slip condition) but the fluid velocity at the surface of the cell equals the cell velocity (U). Therefore changes in the x-velocity u are on the order of U, that is $|\Delta u| \sim U$, and $|\partial u/\partial y| \sim |\Delta u/\Delta y| \sim U/h_0$, where h_0 is a characteristic value of $h(x)$.

The change in fluid velocity as we move through a distance L in the x-direction is likely to be at most U, and therefore $|\partial u/\partial x| \sim U/L$. The continuity equation,

$$\frac{\partial u}{\partial x} + \frac{\partial v}{\partial y} = 0,$$

implies that $|\partial v/\partial y| \sim U/L$; hence $|\Delta v| \sim h_0 U/L$.

Scaling

We nondimensionalise

$$x = Lx^*, \quad y = h_0 y^*, \quad h(x) = h_0 h^*(x^*), \quad u = Uu^*, \quad v = h_0 U v^*/L, \quad p = p_0 p^*,$$

where p_0 is an appropriate scale for the pressure (to be chosen). Note that x^*, y^*, u^*, v^* and p^* are all order 1.

Lubrication theory III

Assuming a steady solution, the nondimensional governing equations are

$$\epsilon^2 Re \left(u^* \frac{\partial u^*}{\partial x^*} + v^* \frac{\partial u^*}{\partial y^*} \right) = - \frac{h_0^2 p_0}{\mu U L} \frac{\partial p^*}{\partial x^*} + \epsilon^2 \frac{\partial^2 u^*}{\partial x^{*2}} + \frac{\partial^2 u^*}{\partial y^{*2}}, \tag{16}$$

$$\epsilon^3 Re \left(u^* \frac{\partial v^*}{\partial x^*} + v^* \frac{\partial v^*}{\partial y^*} \right) = - \frac{h_0^2 p_0}{\epsilon \mu U L} \frac{\partial p^*}{\partial y^*} + \epsilon^3 \frac{\partial^2 v^*}{\partial x^{*2}} + \epsilon \frac{\partial^2 v^*}{\partial y^{*2}}, \tag{17}$$

$$\frac{\partial u^*}{\partial x^*} + \frac{\partial v^*}{\partial y^*} = 0, \tag{18}$$

where $\epsilon = h_0/L \ll 1$ and $Re = UL/\nu$.
We may immediately cancel the viscous terms that have a repeated x^*-derivative since they are much smaller than the viscous terms with a repeated y^*-derivative. Balancing the pressure derivative and viscous terms in the x-component equation (16) leads to the scaling $p_0 = \mu UL/h_0^2$. Multiplying equation (17) by ϵ and simplifying, equations (16) and (17) can be written as

$$\epsilon^2 Re \left(u^* \frac{\partial u^*}{\partial x^*} + v^* \frac{\partial u^*}{\partial y^*} \right) = - \frac{\partial p^*}{\partial x^*} + \frac{\partial^2 u^*}{\partial y^{*2}}, \tag{19}$$

$$0 = - \frac{\partial p^*}{\partial y^*}, \tag{20}$$

where **we have neglected terms of order ϵ^2 and terms of order $\epsilon^3 Re$ relative to the leading-order terms.**

Lubrication theory IV

Solution procedure

- The quantity $\epsilon^2 Re$ is called the **reduced Reynolds number**. We assume it is not too large, which places an upper bound on the possible flux.
- We may immediately solve (20) to find that the pressure is a function of x^* only, that is, **the pressure is constant over the height of the gap**.
- The governing equations are thus (19) and (18), where p^* is a function of x^* only and these must be solved subject to no-slip boundary conditions for u^* at the walls.

Lubrication theory V

Series expansion for small reduced Reynolds number

In the case that the reduced Reynolds number is small, $\epsilon^2 Re \ll 1$ we can use a **series expansion** method to find the velocity, by setting

$$
\begin{aligned}
u^* =& u_0^* + \epsilon^2 Re\, u_1^* + \left(\epsilon^2 Re\right)^2 u_2^* + \dots,\\
v^* =& v_0^* + \epsilon^2 Re\, v_1^* + \left(\epsilon^2 Re\right)^2 v_2^* + \dots,\\
p^* =& p_0^* + \epsilon^2 Re\, p_1^* + \left(\epsilon^2 Re\right)^2 p_2^* + \dots.
\end{aligned}
$$

noting that all the p_i^*'s are independent of y, and then solving for u_0^* (from equation (19)), v_0^* (from equation (18)), u_1^* (from equation (19)), v_1^* (from equation (18)), *etc* in that order. An equation for the pressure can be obtained by integrating the continuity equation over the gap height.

In many cases it is sufficiently accurate to find just the first terms u_0^* and v_0^* (or even just u_0^*).

Generalisation

Note that we could generalise this approach to include:

- dependence upon the third spatial dimension;
- time-dependence of the solution;
- gravity;
- ....

Lubrication theory VI

Example of solution

We consider the domain shown in the figure. For simplicity, we assume two-dimensional flow. We wish to solve the flow in the gap $0 \leq y \leq h(x)$, with $0 \leq x \leq L$.
The flow
is subject to the following boundary conditions:

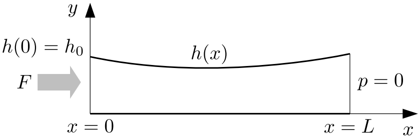

- no-slip at $y = 0$ and $y = h(x)$;
- given
  flux per unit length $F = \int_0^{h_0} u dy$ at $x = 0$;
- given pressure $p = 0$ at $x = L$.

We assume that $h_0 = h(0)$ is a typical value of
the thickness of the domain in the y-direction and
assume that $\epsilon = h_0/L \ll 1$. We can, therefore, apply the lubrication theory.
We scale the variables as follows

$$x^* = \frac{x}{L}, \qquad y^* = \frac{y}{h_0}, \qquad u^* = \frac{u}{U}, \qquad v^* = \frac{v}{\epsilon U},$$

with $U = F/h_0$.

Lubrication theory VII

Assuming that $\epsilon^2 Re \ll 1$, we need to solve the following dimensionless equations (see equations (19), (20) and (18))

$$\frac{\partial^2 u^*}{\partial y^{*2}} - \frac{\partial p^*}{\partial x^*} = 0, \tag{21}$$

$$\frac{\partial p^*}{\partial y^*} = 0, \tag{22}$$

$$\frac{\partial u^*}{\partial x^*} + \frac{\partial v^*}{\partial y^*} = 0, \tag{23}$$

subject to the boundary conditions

$$u^* = v^* = 0 \qquad (y^* = 0), \tag{24}$$

$$u^* = v^* = 0 \qquad [y^* = h^*(x^*)], \tag{25}$$

$$\int_0^1 u^* dy^* = 1 \qquad (x^* = 0), \tag{26}$$

$$p^* = 0 \qquad (x^* = 1). \tag{27}$$

Lubrication theory VIII

Equation (22) imposes that p^* cannot depend on y^*. As a consequence equation (21) can be integrated with respect to y^* and, also using the boundary conditions (24) and (25), we obtain

$$u^*(x^*, y^*) = \frac{1}{2}\frac{dp^*}{dx^*}\left(y^{*2} - h^* y^*\right). \tag{28}$$

In the above expression the term dp^*/dx^* is still an unknown function of x^*.
Using the boundary condition (26) and (28) we find that

$$\left.\frac{dp^*}{dx^*}\right|_{x^*=0} = -12. \tag{29}$$

We now integrate the continuity equation (23) with respect to y^*

$$\int_o^{h^*} \frac{\partial u^*}{\partial x^*} + \frac{\partial v^*}{\partial y^*} dy^* = \cancel{v^*(h^*)} - \cancel{v^*(0)} + \int_o^{h^*} \frac{\partial u^*}{\partial x^*} dy^* = 0,$$

where we have used the no-slip boundary conditions (24) and (25).
Using Leibniz rule[2] and, again, the no-slip boundary conditions (24) and (25) we obtain the following second order equation for the pressure

$$\frac{d}{dx^*}\left(h^{*3}\frac{dp^*}{dx^*}\right) = 0.$$

Lubrication theory IX

From the above equation and using (29) we obtain

$$\frac{dp^*}{dx^*} = -\frac{12}{h^{*3}},$$

which we can plug into equation (28) to obtain the following expression for the velocity in the x^*-direction

$$u^*(x^*, y^*) = -\frac{6}{h^{*3}}\left(y^{*2} - h^* y^*\right).$$

The y^*-component of the velocity can be obtained from the continuity equation (23) and reads

$$v^*(x^*, y^*) = -6\left(-\frac{y^{*3}}{h^{*4}} + \frac{y^{*2}}{h^{*3}}\right)\frac{dh^*}{dx^*}.$$

Finally, the pressure distribution can be obtained by integrating (44) and using the boundary condition (27).

We note that we managed to obtain an analytical expression for the velocity without having to specify the shape of the domain $h^*(x^*)$.

---

[2]

$$\int_{a(z)}^{b(z)} \frac{\partial f(x,z)}{\partial z} dx = \frac{\partial}{\partial z}\int_{a(z)}^{b(z)} f(x,z)dx - f(b,z)\frac{\partial b(z)}{\partial z} + f(a,z)\frac{\partial a(z)}{\partial z}.$$

The Boussinesq approximation for thermally driven flows I

Justification of the Boussinesq approximation

Let us consider a fluid with a weakly variable density and viscosity, so that we can write

$$\rho = \rho_0 \left(1 + \frac{\rho'}{\rho_0}\right), \qquad \nu = \nu_0 \left(1 + \frac{\nu'}{\nu_0}\right), \tag{30}$$

with $\rho'/\rho_o \ll 1$ and $\nu'/\nu_o \ll 1$.
We assume that **fluid flow is generated by buoyant effects.** We fist consider the continuity equation (5), which we write here in index notation

$$\frac{\partial \rho}{\partial t} + \frac{\partial}{\partial x_i}(\rho u_i) = 0. \tag{31}$$

Substituting (30) into (31) we obtain

$$\frac{\partial \rho'}{\partial t} + \left(\rho_0 + \rho'\right) \frac{\partial u_i}{\partial x_i} + u_i \frac{\partial \rho'}{\partial x_i} = 0. \tag{32}$$

We now introduce nondimensional variables as follows

$$x_i^* = \frac{x_i}{L}, \qquad t^* = \frac{tU}{L}, \qquad u_i^* = \frac{u_i}{U}, \tag{33}$$

The Boussinesq approximation for thermally driven flows II

where L is a typical length scale of the problem and U a proper scale for the velocity. Substituting the dimensionless variables (33) into (32) we obtain

$$\frac{\partial}{\partial t^*}\left(\frac{\rho'}{\rho_0}\right)+\left(1+\frac{\rho'}{\rho_0}\right)\frac{\partial u_i^*}{\partial x_i^*}+u_i^*\frac{\partial}{\partial x_i^*}\left(\frac{\rho'}{\rho_0}\right)=0,$$

which shows that, since $\rho'/\rho_0 \ll 1$, at leading order the continuity equation is the same as for an incompressible fluid

$$\frac{\partial u_i^*}{\partial x_i^*}=0.$$

Let us now consider the momentum equation (7), which we again write in index notation, and in which we substitute the expression (30) for the density

$$\rho_0\left(1+\frac{\rho'}{\rho_0}\right)\left(\frac{\partial u_i}{\partial t}+u_j\frac{\partial u_i}{\partial x_j}\right)+\frac{\partial p}{\partial x_i}-\rho_0\nu_0\left(1+\frac{\rho'}{\rho_0}\right)\left(1+\frac{\nu'}{\nu_0}\right)\frac{\partial^2 u_i}{x_j^2}+\rho_0\left(1+\frac{\rho'}{\rho_0}\right)g\hat{z}_i=0, \tag{34}$$

where $\hat{\mathbf{z}}$ is the upward directed vertical unit vector. It is convenient to decomposed the pressure as p_o+p', so that

$$\frac{\partial p_0}{\partial x_i}+\rho_0 g\hat{z}_i=0. \tag{35}$$

The Boussinesq approximation for thermally driven flows III

Substituting (35) into (34) we obtain

$$\rho_0 \left(1+\frac{\rho'}{\rho_0}\right)\left(\frac{\partial u_i}{\partial t}+u_j\frac{\partial u_i}{\partial x_j}\right)+\frac{\partial p'}{\partial x_i}-\rho_0\nu_0\left(1+\frac{\rho'}{\rho_0}\right)\left(1+\frac{\nu'}{\nu_0}\right)\frac{\partial^2 u_i}{\partial x_j^2}+\rho' g\hat{z}_i=0, \qquad (36)$$

We now scale the momentum equation using the following scales for the pressure: $p'=\dfrac{p'}{\rho_0 U^2}$.
With the above assumption the dimensionless version of equation (36) reads

$$\left(1+\frac{\rho'}{\rho_0}\right)\left(\frac{\partial u_i^*}{\partial t^*}+u_j^*\frac{\partial u_i^*}{\partial x_j^*}\right)+\frac{\partial p'^*}{\partial x_i}-\frac{1}{Re}\left(1+\frac{\rho'}{\rho_0}\right)\left(1+\frac{\nu'}{\nu_0}\right)\frac{\partial^2 u_i^*}{\partial x_j^{*2}}+\frac{\rho'}{\rho_0}\frac{1}{F^2}\hat{z}_i=0, \qquad (37)$$

Since we assumed that flow is generated by buoyancy effects, the leading order convective terms have to balance with the gravitational term. Thus we need to have

$$\frac{\rho'}{\rho_0}\frac{1}{F^2}\approx 1.$$

If we now neglect in (37) terms of order ρ'/ρ_0 and ν/ν_0 with respect to terms of order 1 we obtain

$$\frac{\partial u_i^*}{\partial t^*}+u_j^*\frac{\partial u_i^*}{\partial x_j^*}+\frac{\partial p'^*}{\partial x_i}-\frac{1}{Re}\frac{\partial^2 u_i^*}{\partial x_j^{*2}}+\frac{\rho'}{\rho_0}\frac{1}{F^2}\hat{z}_i=0,$$

The Boussinesq approximation for thermally driven flows IV

Writing the continuity and momentum equation back in dimensional form still neglecting small terms, we obtain

$$\frac{\partial u_j}{\partial x_j} = 0, \tag{38a}$$

$$\left(\frac{\partial u_i}{\partial t} + u_j \frac{\partial u_i}{\partial x_j}\right) + \frac{1}{\rho_0}\frac{\partial p}{\partial x_i} - \nu_0 \frac{\partial^2 u_i}{\partial x_j^2} + \left(1 + \frac{\rho'}{\rho_0}\right) g \hat{z}_i = 0. \tag{38b}$$

In other words, at leading order, the only term in which the perturbation of density appears is gravity. This is what is called the **Boussinesq approximation** of the equations of motion.

The Boussinesq approximation for thermally driven flows V

Heat transport equation

When density changes are due to temperature variations, for liquids we can write

$$\rho = \rho_0 \left[1 - \alpha (T - T_0) \right], \tag{39}$$

where α is the **coefficient of thermal expansion.**

In this case the equations of motion have to be coupled with the heat transport equation, which reads

$$\frac{\partial T}{\partial t} + u_j \frac{\partial T}{\partial x_j} - D \frac{\partial^2 T}{\partial x_j^2} = 0,$$

or, in vector form,

$$\frac{\partial T}{\partial t} + \mathbf{u} \cdot \nabla T = D \nabla^2 T,$$

where T denotes temperature and D is the **thermal diffusion coefficient** ($[D] = L^2 T^{-1}$).

Irrotational flows I

Potential function of the velocity

We define the **vorticity** as

$$\boldsymbol{\omega} = \nabla \times \mathbf{u}. \tag{40}$$

In the absence of viscous effects (and introduction of vorticity at the boundaries), it can be shown that vorticity cannot be generated in a moving fluid.
As mentioned, for large values of the Reynolds number, the flow away from the boundaries behaves as if it were inviscid. Therefore, if the vorticity is initially zero, it will remain so at all times (provided there is no mechanism of introduction at the boundaries). In this case the flow is said to be **irrotational**.
We assume

- **incompressible fluid,** and
- **irrotational flow,**

i.e.

$$\nabla \cdot \mathbf{u} = 0, \qquad \nabla \times \mathbf{u} = 0. \tag{41}$$

Note that the conditions (41) are purely kinematic in nature (although they do, of course, affect the dynamic behaviour of the fluid).

Irrotational flows II

Let us consider a closed curve C in an irrotational flow. By Stokes' theorem,

$$\oint_C \mathbf{u} \cdot d\mathbf{x} = \iint_S (\nabla \times \mathbf{u}) \cdot \mathbf{n} dS = \iint_S \boldsymbol{\omega} \cdot \mathbf{n} dS = 0,$$

and thus the **circulation** is zero.
Now consider any two points, say O and P, and any two paths, C_1 and C_2 from O to P through the irrotational flow. Since travelling along C_1 and then back along C_2, is a closed curve through the flow, we must have

$$\oint_{C_1} \mathbf{u} \cdot d\mathbf{x} - \oint_{C_2} \mathbf{u} \cdot d\mathbf{x} = 0 \quad \Rightarrow \quad \oint_{C_1} \mathbf{u} \cdot d\mathbf{x} = \oint_{C_2} \mathbf{u} \cdot d\mathbf{x}.$$

Thus the integral between O and P does not depend on the path of integration, but only on the starting and ending points. This means we can define a function, $\Phi(\mathbf{x})$, which we call the **potential** of the velocity field, such that

$$\Phi(\mathbf{x}) = \Phi_0 + \int_O^P \mathbf{u} \cdot d\mathbf{x}, \tag{42}$$

where Φ_0 is the velocity potential at the point O. In a simply connected region the velocity potential is unique up to the constant Φ_0. Equation (42) implies that we can write

$$\mathbf{u} = \nabla \Phi. \tag{43}$$

Irrotational flows III

The continuity equation for an incompressible fluid, i.e. $\nabla \cdot \mathbf{u} = 0$, together with (43) implies

$$\nabla^2 \Phi = 0. \tag{44}$$

This means **the potential function Φ is harmonic**, that is, it satisfies the Laplace equation. If we solve the problem for the function Φ we can find the velocity $\mathbf{u}$ using equation (43).
The mathematical problem to find an irrotational flow is much easier than that for a rotational flow, for the following main reasons:

- equation (44) is linear, whereas the Navier–Stokes equations are nonlinear;
- the problem is solved for a single scalar function (the potential) rather than multiple functions (the velocity and pressure – four components altogether, which much be solved simultaneously);

From Equation (44), the velocity distribution has the following properties.

- Equation (44) is elliptic, so Φ is smooth, except possibly on the boundary.
- The function Φ is single-valued (as long as the domain is simply connected).

Bernoulli equation for irrotational flows I

If

- **the flow is incompressible,**
- **the flow is irrotational**, and
- **the body force field is conservative**, i.e. $\boldsymbol{\nabla} \times \mathbf{f} = 0$,

then it may be shown that

$$\mathcal{H} = \frac{\partial \Phi}{\partial t} + \frac{|\mathbf{u}|^2}{2} + \frac{p}{\rho} + \Psi = c, \tag{45}$$

where Ψ is the potential of the body force field $\mathbf{f}$, defined as $\mathbf{f} = -\nabla \Psi$, and c is constant. This is the **Bernoulli theorem for irrotational flows**.

Once the velocity field is known, we can use this theorem to find the pressure.

Rheological models for non-Newtonian fluids I

Newtonian incompressible fluids

We recall that for an incompressible Newtonian fluid we can express the stress tensor $\boldsymbol{\sigma}$ as a function of the rate of deformation tensor $\mathbf{e}$ as

$$\boldsymbol{\sigma} = -p\mathbf{I} + 2\mu\mathbf{e}, \tag{46}$$

where p is pressure, $\mathbf{I}$ is the identity tensor, μ is the dynamic viscosity of the fluid and $\mathbf{e}$ is defined as the symmetric part of the velocity gradient tensor $\nabla\mathbf{u}$.

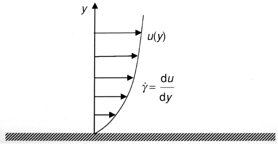

If we refer to a **one-dimensional shear flow** like that reported on the left, with velocity components $[u(y), 0, 0]$ in the directions x the shear stress at any point is given by

$$\sigma_{xy} = \tau = \mu \frac{du(y)}{dy} = \mu\dot{\gamma},$$

where $\dot{\gamma}$ is referred to as **rate of shear strain**.

Rheological models for non-Newtonian fluids II

Newtonian incompressible fluids

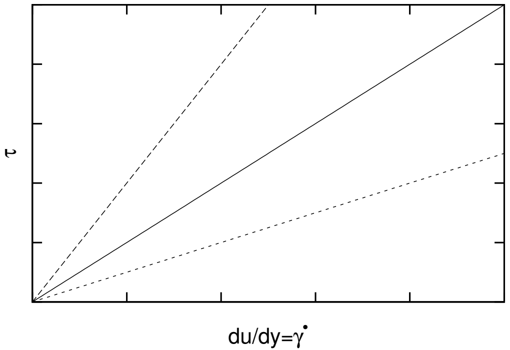

Qualitative dependence of the shear stress τ on the rate of shear strain $\dot{\gamma}$ for three Newtonian fluids with different viscosity.

Time-independent non-Newtonian fluids I

We now consider more complicated behaviours by referring first to the one-dimensional shear flow and then presenting the three-dimensional formulation of the constitutive relationship.
A good reference for non-Newtoninan fluid flow is the book by Tanner (2000).

For **inelastic, non-Newtonian fluids** a possible model for shear behaviour is

$$\dot{\gamma} = f(\tau).$$

The **shear rate** $\dot{\gamma}$ at any point in the fluid is a function of the **shear stress** τ at that point. Fluid behaving in this way are named **non-Newtoninan viscous fluids** or **generalised Newtonian fluids**. They can be distinguished in the following categories:

- **Bingham-Green;**
- **shear thinning** or pseudo-plastic;
- **shear-thickening fluids** or dilatant.

Time-independent non-Newtonian fluids II

Bingham-Green fluids

One-dimensional formulation

In Bingham-Green fluids if the shear stress is below a certain threshold value τ_c no-flow occurs. As the shear stress exceeds such a value the fluid behaves in analogy to a Newtonian fluid.
In one-dimensions we can thus write

$$\tau = \tau_c + \mu\dot{\gamma}.$$

Three-dimensional generalisation

The above constitutive behaviour can be generalised to the three-dimensional case as follows

$$\boldsymbol{\sigma} = -p\mathbf{I} + \left(2\mu + \frac{\tau_c}{\sqrt{-I_{II}}}\right)\mathbf{e}, \tag{47}$$

where I_{II} is the second invariant of the rate of deformation tensor, defined as

$$I_{II} = \frac{1}{2}\left[(tr\mathbf{e})^2 - \left(tr\mathbf{e^2}\right)\right],$$

and, for an incompressible fluid can be written as

$$I_{II} = \frac{1}{2}\mathbf{e} : \mathbf{e}.$$

Time-independent non-Newtonian fluids III

Bingham-Green fluids

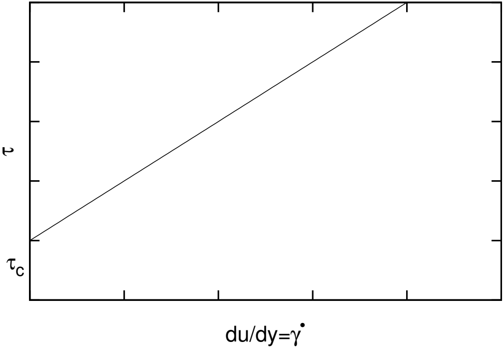

Qualitative dependence of the shear stress τ on the rate of shear strain $\dot{\gamma}$ for a Bingham-Green fluid.

Time-independent non-Newtonian fluids IV

Shear thinning/thickening fluids

One-dimensional formulation

The behaviour of many real fluid is approximately Newtonian in small intervals of the rate of strain but with a viscosity that changes with $\dot{\gamma}$.
This behaviour can often be expressed with good approximation with the following one-dimensional law

$$\tau = \mu_n \left|\dot{\gamma}\right|^n \mathrm{sgn}\left(\dot{\gamma}\right),$$

where the quantity μ_n has the following dimensions: $[\mu_n] = ML^{-1}T^{-2+n}$ and, therefore, is not a viscosity in general. However, it is possible to define an **effective viscosity** μ_{eff}, so that we have

$$\tau = \mu_{eff}\left(\dot{\gamma}\right)\dot{\gamma}.$$

Comparing the above two equations yields the following definition

$$\mu_{eff} = \mu_n \left|\dot{\gamma}\right|^{n-1}.$$

- If the effective viscosity μ_{eff} grows with $\dot{\gamma}$ the fluid is said to be **shear thickening**;
- if the effective viscosity μ_{eff} decreases with $\dot{\gamma}$ the fluid is said to be **shear thinning**.

Three-dimensional generalisation

The above constitutive behaviour can be generalised to the three-dimensional case as follows:

$$\boldsymbol{\sigma} = -p\mathbf{I} + \left(\frac{2^n \mu_n}{\sqrt{-I_{II}}^{1-n}}\right)\mathbf{e}. \qquad (48)$$

Time-independent non-Newtonian fluids V

Shear thinning/thickening fluids

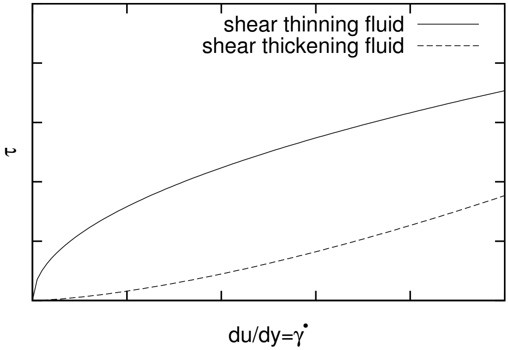

Qualitative dependence of the shear stress τ on the rate of shear strain $\dot{\gamma}$ for a shear thinning and a shear thickening fluid.

Time-independent non-Newtonian fluids VI

Herschel-Bulkley fluids

One-dimensional formulation

The behaviour of fluids carrying particles in suspension can often be expressed superimposing the characteristics of a Bingham-Green fluid with those of a shear thinning/thickening fluid, in the following form:

$$\tau = \left[\tau_c + \mu_n \left|\dot{\gamma}\right|^n\right] \operatorname{sgn}\left(\dot{\gamma}\right).$$

Three-dimensional generalisation

The above constitutive behaviour can be generalised to the three-dimensional case as follows:

$$\boldsymbol{\sigma} = -p\mathbf{I} + \left(\frac{\tau_c}{\sqrt{I_{II}}} + \frac{2^n \mu_n}{\sqrt{-I_{II}}^{1-n}}\right)\mathbf{e}. \tag{49}$$

This is known as a Herschel-Bulkley fluid.

Note that:

- for $\tau_c = 0$ (49) reduces to (47);
- for $n = 1$ (49) reduces to (48);
- for $\tau_c = 0$ and $n = 1$ (49) reduces to (46).

Time-independent non-Newtonian fluids VII

Herschel-Bulkley fluid

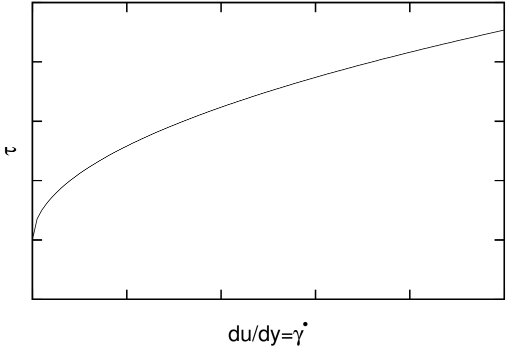

Qualitative dependence of the shear stress τ on the rate of shear strain $\dot{\gamma}$ for a Herschel-Bulkley fluid.

Viscoelastic materials I

In many cases materials display both an **elastic** and **viscous behaviour**.

- In the theory of **linear elasticity** the stress τ in a sheared body is taken proportional to the amount of shear γ;
- in a **Newtonian fluid** shearing stress is proportional to the rate of shear $\dot{\gamma}$.

Stress relaxation

We consider the behaviour of a material in a simple shearing motion, assuming inertia can be neglected.
Suppose the sample is homogeneously deformed, with the amount of shear $\gamma(t)$ variable in time. Let $\tau(t)$ be the corresponding shearing stress.
We consider the **single-step shear history** $\gamma(t) = \gamma_0 H(t)$, with $H(t)$ being the **Heaviside unit step function** ($H(t) = 0$ for $t < 0$, $H = 1$ for $t \geq 0$).

- **Elastic solid:** $\tau(t) = \tau_0 H(t)$, with $\tau_0 = \text{const}$.
- **Newtonian fluid:** since $\tau = \mu\dot{\gamma}$, it would be instantaneously infinite at $t = 0$ and zero for $t > 0$. Then, since

$$\gamma(t) = \frac{1}{\mu}\int_{-\infty}^{t} \tau dt = \gamma_0, \quad (t \geq 0),$$

$$\gamma = 0, \quad (t < 0),$$

τ is a **delta-function with strength** $\mu\gamma_0$.

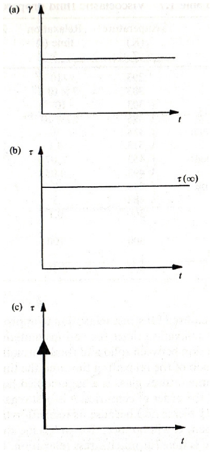

Viscoelastic materials II

Observations on real materials show that the above idealised models are always inaccurate. The stress τ decreases from its initial value to a limiting value τ_∞. The decrease is rapid first and then slows down. This process is called **relaxation**.

- If the limiting value is not zero we say that the material is a **solid;**
- If the limiting value is zero we say that the material is a **fluid.**

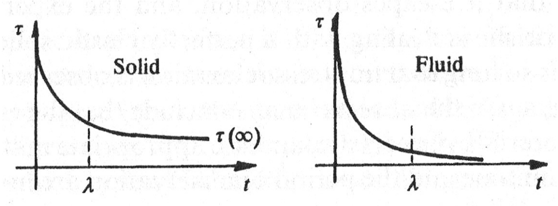

We can define a **relaxation time** λ. This time has to be compared with the **period of observation** T_{obs}.

- If $\lambda/T_{\text{obs}} \ll 1$ one can conclude that the material is a perfectly elastic solid or a viscous fluid, depending on the value of τ_∞;
- if $\lambda/T_{\text{obs}} \gg 1$ one can conclude that the material is a solid;
- if $\lambda/T_{\text{obs}} \approx \mathcal{O}(1)$ we call the material **viscoelastic**.

Viscoelastic materials III

Creep

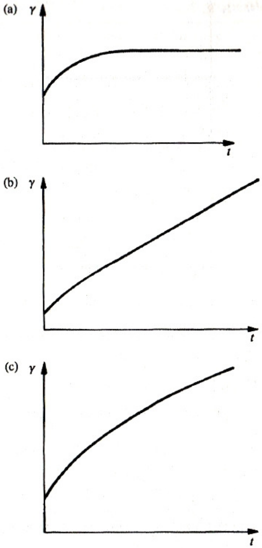

We now consider a **single-step stress history** $\tau(t) = \tau_0 H(t)$.

- **Elastic solid:** $\gamma(t) = \gamma_0 H(t)$, with $\gamma_0 = \text{const}$.
- **Newtonian fluid:** the shear grows at a constant rate, thus $\gamma(t) = \tau_0 t/\mu$, with μ being the dynamic viscosity.

Again, the behaviour of real materials shows departures from these idealised cases. The shear, after an initial possible jump, continues to increase over time.

- If the shear approaches a limiting value γ_∞ the material is said to be a **solid;**
- if the shear grows linearly after a long time the material is said to be a **viscous fluid.**

Viscoelastic materials IV

Response functions

We introduce

- **stress relaxation function** $R(\gamma, t)$: the stress at a time t after the application of a shear step of size γ;
- **creep function** $C(\tau, t)$: the shear at a time t after the application of a stress step of size τ.

The functions R and C are supposed to be zero for $t < 0$.
If the material is isotropic R has to be an odd function of γ and C an odd function of τ.
Assuming that

- R and C are smooth functions,
- γ and τ are small,

we can write

$$R(\gamma, t) = G(t)\gamma + \mathcal{O}(\gamma^3), \qquad C(\tau, t) = J(t)\tau + \mathcal{O}(\tau^3),$$

where we have defined

- $G(t)$ **linear stress relaxation modulus;**
- $J(t)$ **linear creep compliance.**

Viscoelastic materials V

Moreover we define

$$G(0+) = G_g, \qquad J(0+) = J_g, \qquad G(\infty) = G_e \qquad J(\infty) = J_e.$$

Immediately after application of a step in stress/strain ($t = 0+$) we have

$$\tau = G_g \gamma, \qquad \gamma = J_g \tau,$$

therefore we have

$$G_g J_g = 1.$$

Viscoelastic materials VI

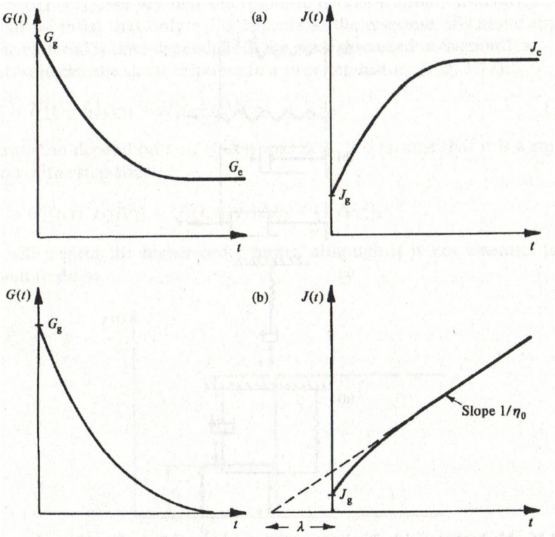

Relaxation modulus G and creep compliance J for (a) solids and (b) fluids.

Viscoelastic materials VII

Spring-dashpot models

It is useful to consider idealised models consisting of combinations of **springs** and **dashpots** to interpret the behaviour of complex viscoelastic materials.

- **Spring.** The spring obeys the simple relationship $\tau = k\gamma$. For the spring we have

$$G(t) = kH(t), \qquad J(t) = \frac{1}{k}H(t).$$

- **Dashpot**. This is a viscous element so that $\dot{\gamma} = \tau/\mu$. For the dashpot the following relationships hold

$$G(t) = \mu\delta(t), \qquad J(t) = t\frac{H(t)}{\mu}.$$

Dashpots and springs can be combined with the following rules

- when two elements are **combined in series their compliances are additive;**
- when two elements are **combined in parallel their moduli are additive.**

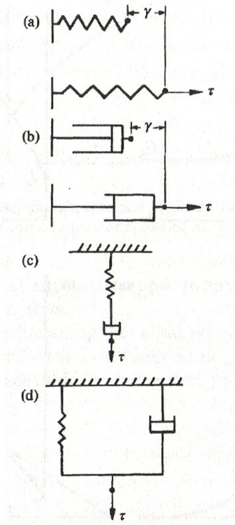

Viscoelastic materials VIII

Examples

Maxwell element

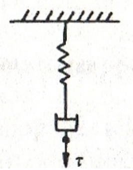

A Maxwell element consists of a spring and a dashpot in series. The creep compliance is therefore

$$J(t) = \left(\frac{1}{k} + \frac{t}{\mu}\right) H(t).$$

Kelvin-Meyer element

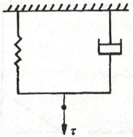

A Kelvin-Meyer element consists of a spring and a dashpot in parallel. The relaxation modulus is therefore

$$G(t) = kH(t) + \mu\delta(t).$$

Viscoelastic materials IX

Superposition of multiple steps

Knowledge of the single-step response functions $G(t)$ and $J(t)$ allows one to predict the **response to any input** within the linear range, i.e. when stresses proportional to γ^3 and strains proportional to τ^3 can be neglected.

We first note that the response is **invariant to time translations**, so that

$$\gamma(t) = \gamma_0 H(t - t_0) \quad \Rightarrow \quad \tau(t) = \gamma_0 G(t - t_0).$$

We now consider a 2-step shear history

$$\gamma(t) = H(t - t_1)\Delta\gamma_1 + H(t - t_2)\Delta\gamma_2.$$

In general the corresponding stress can depend on t, t_1, t_2, $\Delta\gamma_1$ and $\Delta\gamma_2$. We assume that it is a smooth function of the step sizes and expand it as follows

$$\tau(t) = G_1(t, t_1, t_2)\Delta\gamma_1 + G_2(t, t_1, t_2)\Delta\gamma_2 + \mathcal{O}(\Delta\gamma^3).$$

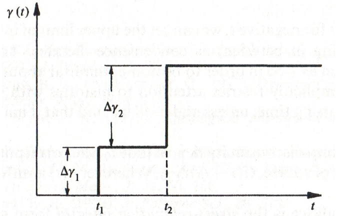

Since the above expression also has to hold for $\Delta\gamma_1 = 0$ and $\Delta\gamma_2 = 0$ it follows that $G_i = G(t - t_i)$, with $i = 1, 2$. Generalising ot N steps at the times t_n we obtain

$$\gamma(t) = \sum_{n=1}^{N} H(t - t_n)\Delta\gamma_n \quad \Rightarrow \quad \tau(t) = \sum_{n=1}^{N} G(t - t_n)\Delta\gamma_n.$$

Viscoelastic materials X

Passing to the limit in the above sums we obtain that the shear history can be written as

$$\gamma(t) = \int_0^t H(t-t')d\gamma(t'),$$

and the stress in time as

$$\tau(t) = \int_{-\infty}^t G(t-t')d\gamma(t'). \tag{50}$$

This is called the **stress relaxation integral**.

Important notes

- Since $G(t) = 0$ for $t < 0$ the upper limit in the integral can be arbitrarily chosen in the range $[t, \infty)$.
- Assuming $\gamma(t)$ is differentiable, we have $d\gamma(t) = \dot{\gamma}(t)dt$.

Following analogous steps we could consider the following stress history

$$\tau(t) = \int_0^t H(t-t')d\tau(t'),$$

and obtain the **creep integral** as

$$\gamma(t) = \int_{-\infty}^t J(t-t')d\tau(t').$$

Viscoelastic materials XI

Linear viscoelastic behaviour

A suitable three-dimensional extension of equation (50) is given by

$$\sigma_{ij} + p\delta_{ij} = d_{ij} = \int_{-\infty}^{t} 2G(t - t')e_{ij}(t')dt', \qquad (51)$$

where d_{ij} is the deviatoric part of the stress tensor and e_{ij} is the rate of strain tensor.

Note: for a Newtonian fluid we have $G(t - t') = \mu\delta(t - t')$ and therefore

$$\sigma_{ij} + p\delta_{ij} = d_{ij} = \int_{-\infty}^{t} 2\mu\delta(t - t')e_{ij}(t')dt' = 2\mu e_{ij}(t),$$

which agrees with equation (46).

Viscoelastic materials XII

Sinusoidal viscoelastic response

A commonly used procedure to test rheological properties of viscoelastic fluids consists of applying to the material a time-sinusoidal strain of small amplitude, so that

$$\gamma = \hat{\gamma} e^{i\omega t} + c.c., \qquad \dot{\gamma} = i\omega\hat{\gamma} e^{i\omega t} + c.c. \tag{52}$$

with $\hat{\gamma} \ll \pi$. Under the assumption of linear behaviour of the system, following from the assumption $\hat{\gamma} \ll \pi$, the shear modulus can be written as

$$\tau = \hat{\tau} e^{i\omega t} + c.c.$$

Substituting (52) into (50) (and omitting the complex conjugates) we obtain

$$\hat{\tau} e^{i\omega t} = i\omega\hat{\gamma} \int_{-\infty}^{t} G(t - t') e^{i\omega t'} dt'.$$

We define the **complex modulus** G^* as $\hat{\tau}/\hat{\gamma}$. From the above equation, setting $s = t - t'$, we obtain

$$G^* = G' + iG'' = i\omega \int_0^\infty G(s) e^{-i\omega s} ds. \tag{53}$$

Separating in (53) the real and imaginary parts we find

$$G^* = G' + iG'' = \int_0^\infty \omega G(s) \sin(\omega s) ds + i \int_0^\infty \omega G(s) \cos(\omega s) ds.$$

with

Viscoelastic materials XIII

- $G'(\omega)$ is the **storage modulus;**
- $G''(\omega)$ is the **loss modulus.**

It is also possible to define the **complex viscosity** as

$$\mu^* = \frac{\hat{\tau}}{\hat{\dot{\gamma}}} = \mu' - i\mu'' = \frac{G^*}{i\omega} = \frac{G''}{\omega} - i\frac{G'}{\omega}. \tag{54}$$

Note that $\mu' = G''/\omega$ is the equivalent of the dynamic viscosity for a Newtonian fluid.

If we record with and an experiment $\gamma(t)$ and $\tau(t)$ we have a phase shift δ between the two signals. If $G'' = 0$ the phase shift is zero ($\delta = 0$). In particular we have

$$\tan\delta = \frac{G''}{G'}.$$

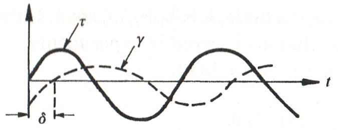

Viscoelastic materials XIV

Solution of sinusoidally oscillating linear flows of a viscoelastic fluid

The equation of motion is given by the Cauchy equation (7) and the continuity equation (6)

$$\rho\left(\frac{\partial \mathbf{u}}{\partial t} + (\mathbf{u}\cdot\nabla\mathbf{u})\right) = \nabla\cdot\boldsymbol{\sigma}, \tag{55}$$

$$\nabla\cdot\mathbf{u} = 0, \tag{56}$$

Substituting (51) into (55) and **neglecting quadratic terms in the velocity**, we obtain

$$\rho\frac{\partial \mathbf{u}}{\partial t} = -\nabla p + \int_{-\infty}^{t} G\left(t-t'\right)\nabla^2\mathbf{u}\,dt'. \tag{57}$$

Assuming a sinusoidally oscillating flow we can set $\mathbf{u}(\mathbf{x},t) = \hat{\mathbf{u}}(\mathbf{x})e^{i\omega t} + c.c.$ and $p(\mathbf{x},t) = \hat{p}(\mathbf{x})e^{i\omega t} + c.c.$, and substituting into (57), also making use of (53) and (54), we obtain

$$\rho i\omega\hat{\mathbf{u}} = -\nabla\hat{p} + \mu^*\nabla^2\hat{\mathbf{u}}, \tag{58}$$

$$\nabla\cdot\hat{\mathbf{u}} = 0. \tag{59}$$

In other words the problem to solve is the same as that for a Newtonian fluid under the same conditions, provided the fluid viscosity μ is replaced with the complex viscosity μ^*.

Flow in the posterior chamber

Flow of aqueous humour: Why is there flow? I

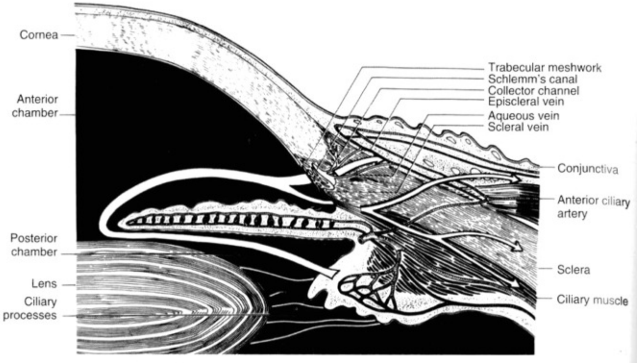

The aqueous flow has two main roles:

- Provides the cornea and the lens (avascular tissues) with nutrients
- Maintains balance between aqueous production and drainage. Outflow resistance regulates the **intraocular pressure (IOP).**

- Nutrition of the cornea and lens is mainly achieved through flow of the aqueous humour.

Flow of aqueous humour: Why is there flow? II

- There is bulk flow from ciliary processes through the pupil (radially inward) and then radially outward to the trabecular meshwork and Schlemm's canal and out of the eye.
- In addition, there is a **temperature gradient across the anterior chamber:**
  - at the back of the anterior chamber the temperature is close to the core body temperature ($\sim 37^\circ$);
  - the outside of the cornea is exposed to ambient conditions (perhaps $\sim 20^\circ$);
  - even though the temperature on the inside wall is close to 37°, there is a significant difference between the temperature at the front and that at the back.

  Therefore **buoyancy effects give rise to an additional flow.**
- The latter flow is particularly relevant when there is particulate matter in the anterior chamber.

Motivation for studying aqueous humour flow I

Red blood cells

- **Red blood cells** are not normally found in the anterior chamber.
- Occur when there is rupture of blood vessels in the eye.
- Two forms:
  - **fresh cells** (less than 4 months old) can deform substantially and squeeze through the drainage system of the eye;
  - **ghost cells** (older than 4 months) are stiffer and cannot exit the eye. This may cause an increase in intraocular pressure as drainage pathways become blocked. Their density is significantly higher than that of water (~ 1500 kg/m^3). May cause sediment at the bottom of the anterior chamber **(hyphema)**.

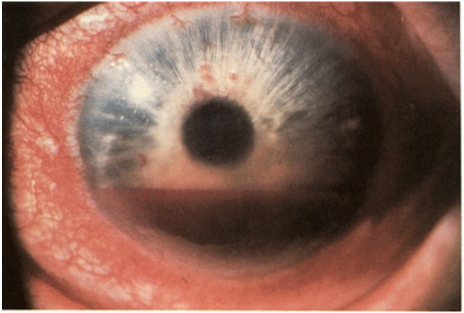

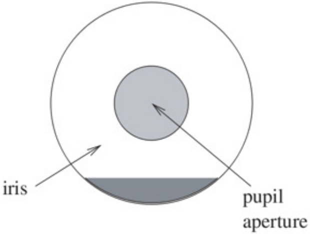

Motivation for studying aqueous humour flow II

White blood cells

- White blood cells may also be present, typically indicating an inflammatory state of the ciliary body.
- The cells aggregate, forming the so-called **keratic precipitates**, shown below.

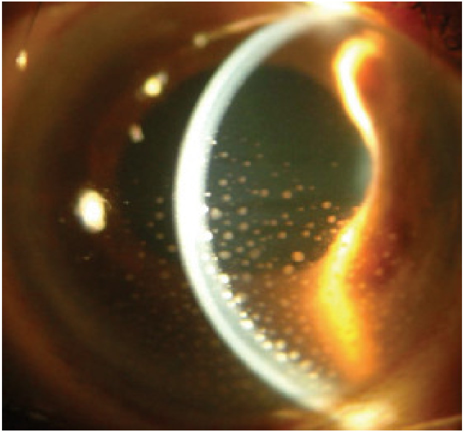

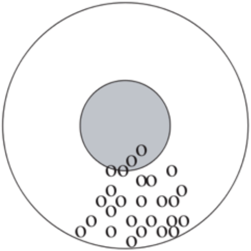

Motivation for studying aqueous humour flow III

Glaucoma

- **Glaucoma** results in slow **progressive damage to the optic nerve** and subsequent loss of vision.
- Risk factors include:
  - **elevated eye pressure;**
  - increased age;
  - previous ocular injury.

  The only treatable risk factor is elevated eye pressure.

- Characteristics
  - Rate of production of aqueous humour remains constant.
  - The resistance to drainage increases (although the causes of this are not well understood).
  - Result is increase in intraocular pressure.
- Two types:
  - **open-angle glaucoma:** more common, when drainage becomes blocked.
  - **closed-angle glaucoma:** when flow from the posterior to the anterior chambers is blocked.

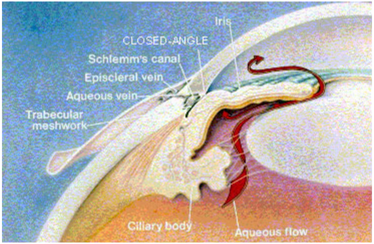

Closed angle glaucoma (Wolfe Eye Clinic)

Geometry and coordinate system

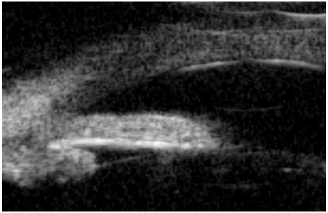

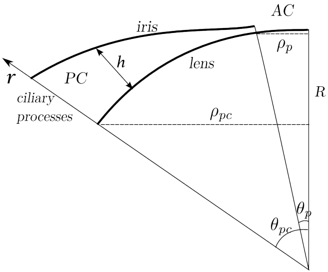

Figure : Left: ultrasound scan image of the posterior chamber. Right: coordinate system and notation.

- The geometry is taken from high frequency ultrasound scans.
- We can split the domain in two regions: **posterior chamber** and **iris–lens channel.**
- Both regions are "long" and "thin". We therefore use **lubrication theory.**
- We adopt a system of spherical coordinates (r, θ, ϕ) and the corresponding velocity components are denoted with $\mathbf{u} = (u_r, u_\theta, u_\phi)$.
- The domain chamber lies within the boundaries $R < r < R + h(\theta)$, $\theta_p < \theta < \theta_{pc}$, $0 \leq \phi \leq 2\pi$.
- The aqueous humour is treated as a Newtonian fluid with density ρ and viscosity ν.

Scaling I

Geometric length scales

- The width of the posterior chamber $L = R(\theta_{pc} - \theta_p)$ is comparable with curvature of the lens R, which we therefore can use as a lengthscale in (θ, ϕ) direction.
- The average height of the domain $h_a = \frac{R}{L} \int_{\theta_p < \theta < \theta_{pc}} h(\theta) d\theta$ is used as lengthscale in the radial (across the chamber) direction.
- We define the aspect ratio of the domain as $\epsilon = h_a/R$. In the real case $\epsilon \lessapprox 0.1$

Velocity scale

- **Production/drainange flow.** We denote the flux as of aqueous procuced at the ciliary processes as F. ciliary processes.
- **Flow induced during iris motion.** During pupil dilation/contraction we assume that the iris moves with a prescribed velocity $\mathbf{v} = (v_r, v_\theta, v_\phi)$ and the volume of the posterior chamber varies by ΔV. The aqueous flux through the pupil is $F_i = \Delta V/T$, where T is the time of iris motion.
  - Pupil constriction lasts less than one second.
  - Pupil dilation takes place over several seconds.
- We define the case of the velocity in the θ and ϕ directions as $U = \tilde{F}/(2\pi \sin\theta_{pc} h_{pc}(R + h_{pc}/2))$, where $\tilde{F} = F$ for the fixed iris case and $\tilde{F} = F_i$ during iris motion.
- The velocity in the r-direction is scaled with ϵU.

Scaling II

- The **reduced Reynolds number** $Re_{\mathrm{red}} = \epsilon^2 RU/\nu$ is much smaller than one in all cases, justifying the lubrication theory approximation.
- For the case of pupil expansion/contraction we can use the **quasi-steady approximation for the flow.**

Governing equations

After simplifying the Navier-Stokes equations using the lubriation theory we find the following set of equations

$$\nabla_h p = \mu \frac{1}{r^2} \frac{\partial}{\partial r}\left(r^2 \frac{\partial \mathbf{u}_h}{\partial r}\right), \tag{60a}$$

$$\nabla_h \cdot \mathbf{u}_h + \frac{1}{r^2} \frac{\partial (r^2 u_r)}{\partial r} = 0, \tag{60b}$$

where p is independent of r, and 'h' is a subscript indicating that only the (θ, ϕ)-components are considered (and not the r-component).

Boundary conditions

- No slip condition at the lens and iris (that can move);
- given flus at the ciliary processes;
- given pressure at the pupil.

Solution

- The solution to (60a), subject to no-slip boundary conditions, is

$$\mathbf{u}_h = \frac{1}{2\mu}\boldsymbol{\nabla}_h p\Big(r^2 + R(R+h(\theta)) - r(2R+h(\theta))\Big) + \mathbf{v}_h \frac{R+h}{h}\Big(1-\frac{R}{r}\Big), \qquad (61)$$

  where $\mathbf{v}_h$ is the (θ, ϕ)-components of $\mathbf{v}$ (or zero in the case with no miosis).

- Integrating continuity equation (60b) with respect to r and using the no-slip conditions $u_r = 0$ at $r = R$ and $u_r = v_r$ at $r = R + h$, we obtain a governing equation for the pressure

$$\frac{1}{12\mu}\boldsymbol{\nabla}_h \cdot (h^3 \boldsymbol{\nabla}_h p) = v_r + \frac{h}{2(R+h)}\boldsymbol{\nabla}_h \cdot \Big((R+h)\mathbf{v}_h\Big) - \frac{1}{2}\boldsymbol{\nabla}_h h \cdot \mathbf{v}_h, \qquad (62a)$$

$$\frac{F}{\pi \sin\theta} = \frac{\partial p}{\partial \theta}\frac{h^3}{6\mu} - (R+h)hv_\theta \qquad (\theta = \theta_{pc}), \qquad (62b)$$

$$p = 0 \qquad (\theta = \theta_p). \qquad (62c)$$

Results I

Production/drainage flow

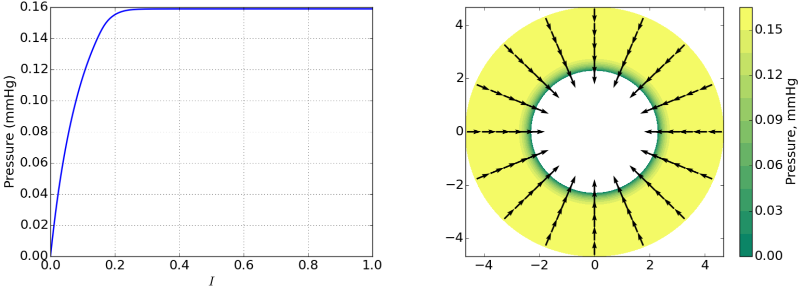

(a) (b)

Figure : (a) Pressure distribution along the posterior chamber, $l = 0$ corresponds to the position of the pupil and $l = 1$ to the ciliary body. (b) View on the posterior chamber from the top. Colors represent pressure and arrows show the normalised velocity vectors.

Results II

Flow during miosis

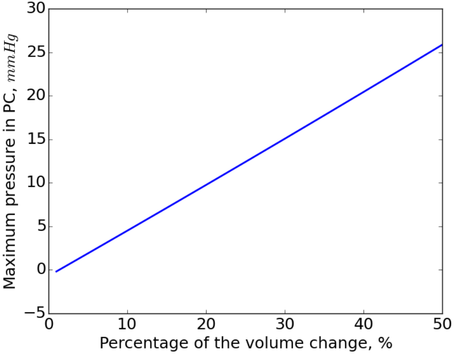

Figure : Maximum pressure as a function of the percentage of posterior chamber volume change after the contraction. Time of the contraction is 1 second.

Results III

Partial pupillary block

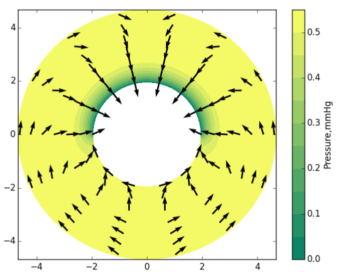

(a)

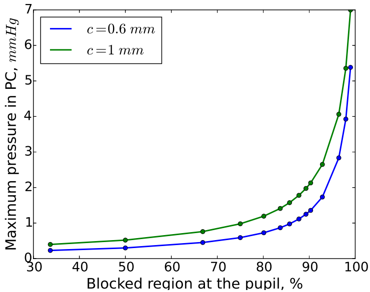

(b)

Figure : (a) Pressure distribution along the posterior chamber and normalized velocity vectors in the case of a partial pupil block. (b) Maximim pressure as a fuction of the percentage of blocked pupil for different lengths of the iris-lens channel.

Flow in the anterior chamber

Thermal flow between infinitely long parallel plates I

As a simple introductory example to understand the flow induced by thermal effects in the anterior chamber of the eye we consider the problem depicted in the figure below. A two-dimensional steady flow is generated in the space between two infinitely long parallel plates, kept at different temperatures (T_0 and T_1, respectively). The two plates are at a distance h between one another. We assume that gravity acts in the positive x-direction.

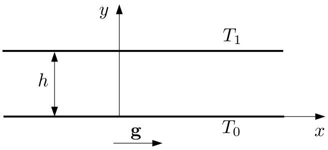

We study the motion of the fluid adopting Boussinesq approximation (see page 53). Owing to the infinite dimension of the domain in the x-direction we seek solutions such that

$$\mathbf{u} = [u(y), 0], \qquad \frac{\partial T}{\partial x} = 0.$$

Under the above assumptions the equations of motion and the corresponding boundary conditions read

$$-\frac{1}{\rho_0}\frac{\partial p}{\partial x} + \nu\frac{\partial^2 u}{\partial y^2} + g\left[1 - \alpha(T - T_0)\right] = 0, \qquad (63a)$$

Thermal flow between infinitely long parallel plates II

$$\frac{\partial p}{\partial y} = 0, \tag{63b}$$

$$\frac{\partial^2 T}{\partial y^2} = 0, \tag{63c}$$

$$u = 0 \qquad (y = 0, h), \tag{63d}$$

$$T = T_0 \qquad (y = 0), \tag{63e}$$

$$T = T_1 \qquad (y = h). \tag{63f}$$

Note that the continuity equation is automatically satisfied.
From equation (63c) with boundary conditions (63e) and (63f) we obtain

$$T = T_0 + \eta y, \qquad \eta = \frac{T_1 - T_0}{h}.$$

From equation (63b) we infer that p does not depend on y. We can therefore integrate (63a) with respect to y and, imposing the boundary conditions (63d), we obtain

$$u = \frac{1}{2\nu}\left(\frac{1}{\rho_0}\frac{\partial p}{\partial x} - g\right) y(y-h) + \frac{g\alpha\eta}{6\nu} y\left(y^2 - h^2\right). \tag{64}$$

Since we have assumed $\partial u/\partial x = 0$, (64) implies that $\partial^2 p/\partial x^2 = 0$ and therefore $\partial p/\partial x = \text{const}$.

Thermal flow between infinitely long parallel plates III

In order to determine $\partial p/\partial x$ we note that, for symmetry reasons, the net flux in the x-direction must vanish. Hence, we impose

$$\int_0^h u dy = 0,$$

and finally obtain

$$p = \rho_0 g \left[1 - \frac{\alpha}{2}(T_1 - T_0)\right] x + c,$$

$$u = \frac{g\alpha}{6\nu h}\,(T_1 - T_0)\, y \left(y - \frac{h}{2}\right)(y - h),$$

where c is an arbitrary constant. As expected for symmetry reasons, the velocity vanishes at $y = 0$, $y = h/2$ and $y = h$.

Thermal flow between infinitely long parallel plates IV

This solution is plotted in terms of normalised variables in the following figure

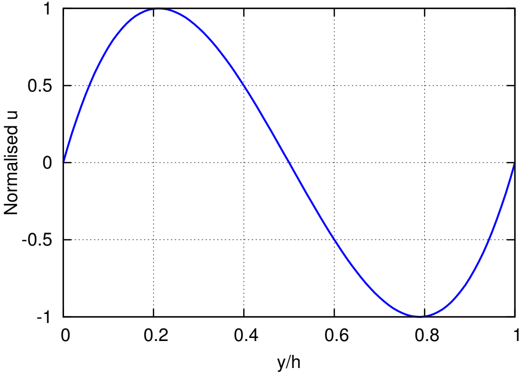

Analytical model of aqueous humour flow I

The generation of thermally riven flows in the anterior chamber has been studied by various authors:

- Canning et al. (2002), Fitt and Gonzalez (2006): **analytical models.**
- Heys et al. (2001), Heys and Barocas (2002) **fully numerical model.**
- ...

In the following we briefly present the models by Canning et al. (2002) and Fitt and Gonzalez (2006).

Geometry

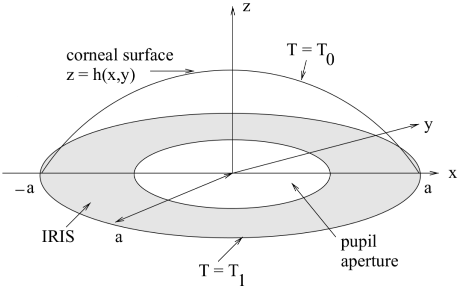

Sketch of the geometry. Note that gravity acts along the positive x-axis.

Analytical model of aqueous humour flow II

Governing equations

We use **Boussinesq approximation** to model density changes due to thermal effects. Thus, according to equation (39), we write

$$\rho = \rho_0 \left(1 - \alpha \left(T - T_0\right)\right).$$

We recall that, according to Boussinesq's approximation (see 53), since density and viscosity changes are small we can replace ρ with ρ_0 in all terms of the Navier-Stokes equation, except the gravitational one, and assume that the kinematic viscosity is constant (ν_0).
We thus need to solve the following system of equations

$$\rho_0 \left(\frac{\partial \mathbf{u}}{\partial t} + (\mathbf{u} \cdot \nabla \mathbf{u})\right) = -\nabla p + \rho_0 \nu_0 \nabla^2 \mathbf{u} + \rho_0 \left(1 - \alpha \left(T - T_0\right)\right) \mathbf{g},$$

$$\nabla \cdot \mathbf{u} = 0,$$

$$\frac{\partial T}{\partial t} + \mathbf{u} \cdot \nabla T = D \nabla^2 T,$$

subjected to the boundary conditions

$$u = v = w = 0, \qquad T = T_1 \qquad (z = 0),$$

$$u = v = w = 0, \qquad T = T_0 \qquad (z = h),$$

with u, v and w the x, y and z components of the velocity, respectively.

Analytical model of aqueous humour flow III

Simplification using lubrication theory

- We define $\epsilon = h_0/a$ (anterior–posterior chamber depth divided by radius).
- Typically $\epsilon^2 \approx 0.06$, motivating the limit of small ϵ.
- We use the lubrication theory to simplify the equations, as described at page 44. In particular we neglect terms of order ϵ^2, $\epsilon^2 Re$ and $\epsilon^2 RePr$ with respect to terms of order 1, where we have defined:

Reynolds number $$Re = \frac{Ua}{\nu_0},$$

Prandtl number $$Pr = \frac{\nu_0}{D},$$

and U is a characteristic scale of the velocity.

Analytical model of aqueous humour flow IV

The reduced system of equations

The simplified equations read:

$$
\begin{aligned}
&x\textbf{-momentum:} && -\frac{1}{\rho_0}\frac{\partial p}{\partial x} + \nu_0 \frac{\partial^2 u}{\partial z^2} + g\left(1 - \alpha\left(T - T_0\right)\right) = 0,\\
&y\textbf{-momentum:} && -\frac{1}{\rho_0}\frac{\partial p}{\partial y} + \nu \frac{\partial^2 v}{\partial z^2} = 0,\\
&z\textbf{-momentum:} && \frac{\partial p}{\partial z} = 0,\\
&\textbf{Continuity} && \frac{\partial u}{\partial x} + \frac{\partial v}{\partial y} + \frac{\partial w}{\partial z} = 0,\\
&\textbf{Diffusion} && \frac{\partial^2 T}{\partial z^2} = 0.
\end{aligned}
$$

Analytical model of aqueous humour flow V

This system of equations can be solved analytically (for any domain shape h), following a procedure very similar to that described at page 49. The following solution is obtained

$$
\begin{aligned}
u &= -\frac{(T_1 - T_0) g \alpha z}{12 \nu h} (2z - h)(z - h) \\
v &= 0 \\
w &= -\frac{(T_1 - T_0) g \alpha z^2}{24 \nu h^2} \frac{\partial h}{\partial x} (z^2 - h^2) \\
p &= p_0 + (x + a)\, g \rho_0 \left(1 - \frac{\alpha (T_1 - T_0)}{2}\right)
\end{aligned}
$$

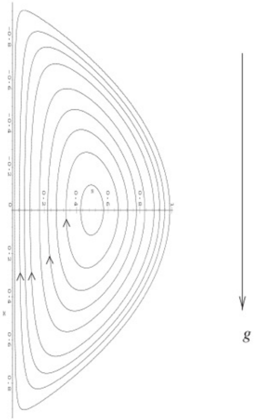

- The **flow is two-dimensional**, as it takes place on planes defined by the equation $y = \text{const}$.
- The **maximum velocity**, computed with realistic values of all parameters, is estimated to be $1.98 \times 10^{-4} (T_1 - T_0)$ m/s/K, which **is consistent with experimental observations**.
- The **solution allows us to compute many other physically meaningful quantities**, *e.g.* the wall shear stress on the surface.

Numerical simulations I

Fully numerical solutions have also been proposed in the literature, e.g. Heys et al. (2001); Heys and Barocas (2002).

Modelling assumptions:

- **Fully numerical approach.**
- The aqueous is modelled as a Newtonian fluid.
- Axisymmetric flow (Heys et al., 2001), fully thee-dimensional flow (Heys and Barocas, 2002).
- Linear elastic behaviour of the iris.

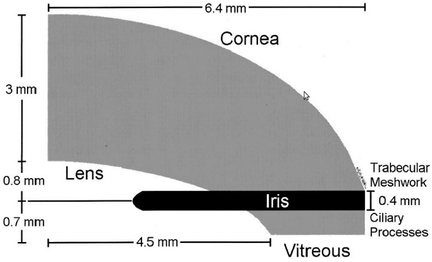

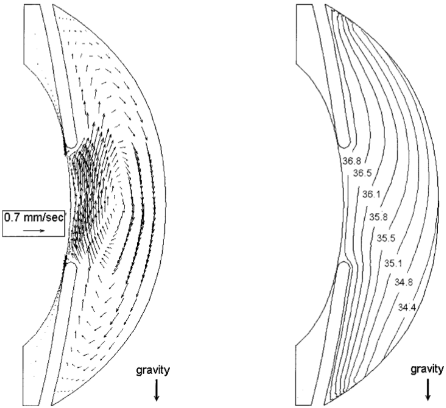

Velocity and temperature fields (from Heys and Barocas, 2002).

Numerical simulations II

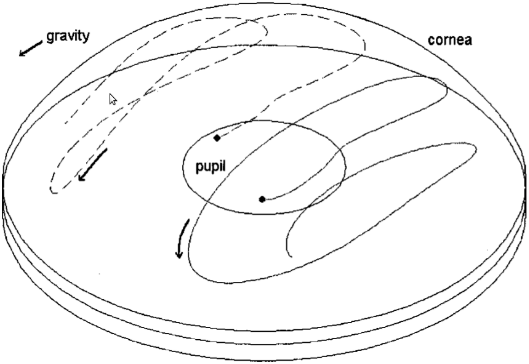

Three-dimensional particle paths (from Heys and Barocas, 2002).

Numerical simulations III

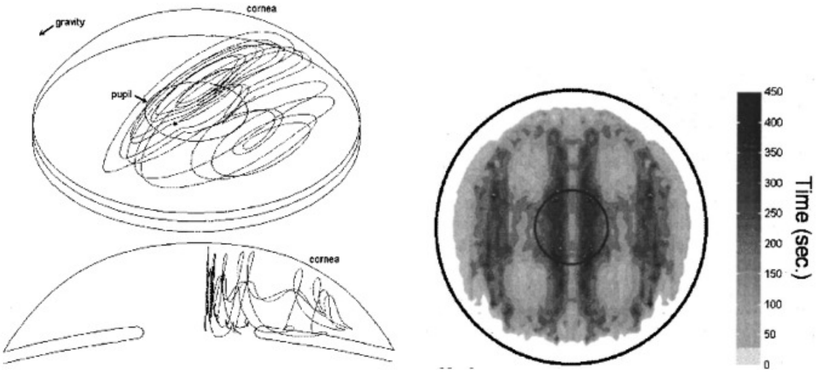

Three-dimensional particle paths and residence times (from Heys and Barocas, 2002).

Fluid dynamics of the vitreous chamber

Vitreous characteristics and functions

Vitreous composition

The main constituents are

- Water (99%);
- hyaluronic acid (HA);
- collagen fibrils.

Its structure consists of long, thick, non-branching collagen fibrils suspended in hyaluronic acid.

Normal vitreous characteristics

- The healthy vitreous in youth is a gel-like material with **visco-elastic mechanical properties**, which have been measured by several authors (Lee et al., 1992; Nickerson et al., 2008; Swindle et al., 2008).
- In the outermost part of the vitreous, named **vitreous cortex**, the concentration of collagen fibrils and HA is higher.
- The vitreous cortex is in contact with the **Internal Limiting Membrane (ILM)** of the retina.

Physiological roles of the vitreous

- **Support function for the retina** and filling-up function for the vitreous body cavity;
- **diffusion barrier** between the anterior and posterior segment of the eye;
- establishment of an **unhindered path of light.**

Vitreous ageing

With advancing age the vitreous typically undergoes significant changes in structure.

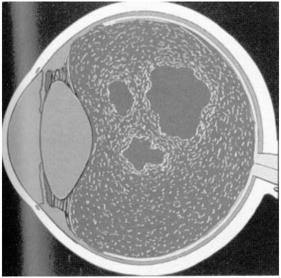

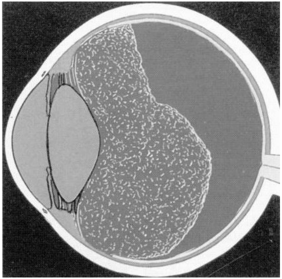

- Disintegration of the gel structure which leads to **vitreous liquefaction (synchisys)**. This leads to an approximately linear increase in the volume of liquid vitreous with time. Liquefaction can be as much extended as to interest the whole vitreous chamber.
- Shrinking of the vitreous gel **(syneresis)** leading to the detachment of the gel vitreous from the retina in certain regions of the vitreous chamber. This process typically occurs in the posterior segment of the eye and is called **posterior vitreous detachment (PVD)**. It is a pathophysiologic condition of the vitreous.

Vitreous replacement

After surgery **(vitrectomy)** the vitreous may be completely replaced with tamponade fluids:

- silicon oils water;
- aqueous humour;
- perfluoropropane gas;
- . . .

Partial vitreous liquefaction

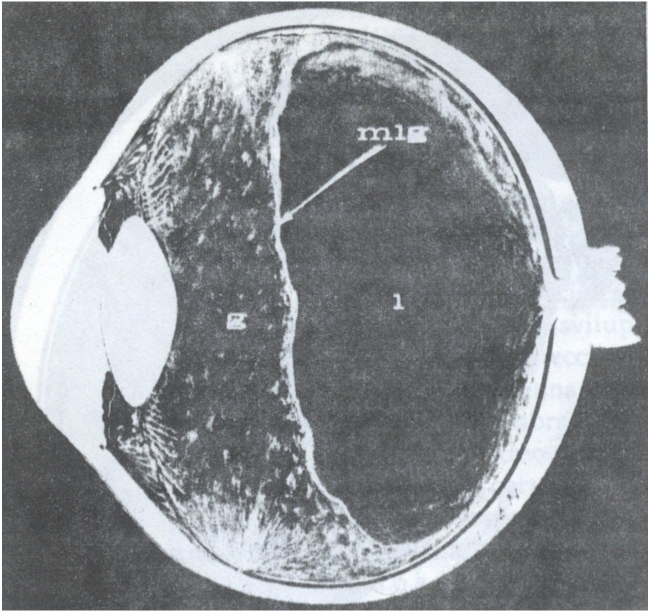

Motivations of the work

Why research on vitreous motion?

- Possible connections between the mechanism of **retinal detachment** and
  - the shear stress on the retina;
  - flow characteristics.
- Especially in the case of liquefied vitreous eye rotations may produce effective **fluid mixing**. In this case **advection may be more important that diffusion** for mass transport within the vitreous chamber.
  Understanding diffusion/dispersion processes in the vitreous chamber is important to predict the behaviour of drugs directly injected into the vitreous.

Retinal detachment

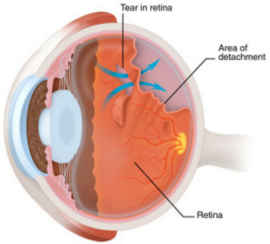

Posterior vitreous detachment and vitreous degeneration:

- more common in myopic eyes;
- preceded by changes in vitreous macromolecular structure and in vitreoretinal interface $\rightarrow$ possibly mechanical reasons.

- If the retina detaches from the underlying layers $\rightarrow$ loss of vision;
- Rhegmatogeneous retinal detachment: fluid enters through a retinal break into the subretinal space and peels off the retina.
- **Risk factors:**
  - **myopia;**
  - posterior vitreous detachment (PVD);
  - lattice degeneration;
  - ...

Scleral buckling

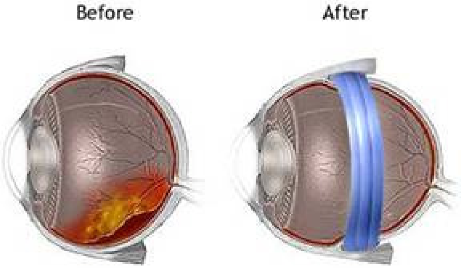

Scleral buckling is the application of a rubber band around the eyeball at the site of a retinal tear in order to promote re-attachment of the retina.

Intravitreal drug delivery

It is difficult to transport drugs to the retina from 'the outside' due to the tight blood-retinal barrier → use of **intravitreal drug injections.**

Saccadic eye rotations

Saccades are eye movements that rapidly redirect the eyes from one target to another
The main characteristics of a saccadic eye movement are (Becker, 1989):

- an **extremely intense angular acceleration** (up to 30000 deg/s2);
- a comparatively less intense deceleration which is nevertheless able to induce a very fast arrest of the rotation
- an **angular peak velocity** increasing with the saccade amplitude up to a saturation value **ranging between 400 - 600 deg/s**.

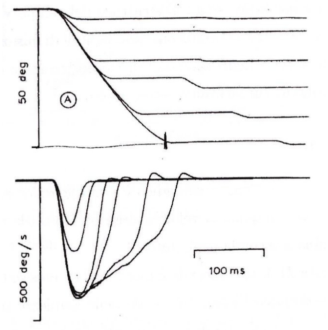

The maximum amplitude of a saccade is about 50° though most eye rotations have amplitudes smaller than 20°. Saccade duration and amplitude are related and the duration is at most of the order of a tenth of a second.

Unidirectional motion of a viscoelastic fluid I

We start by considering a very simple unidirectional flow. Even if the flow in the eye is obviously not unidirectional this analysis allows us to discuss some important characteristics of the flow in the vitreous chamber.
We consider the flow of a homogeneous and viscoelastic fluid within a gap between two parallel walls, located at $y = 0$ and $y = d$.

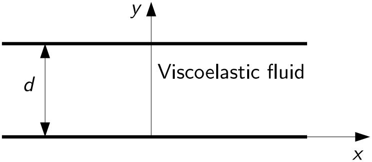

The unidirectional flow under consideration is governed by the following equation

$$\rho \frac{\partial u}{\partial t} + \int_{-\infty}^{t} G(t - t') \frac{\partial^2 u}{\partial y^2} dt' = 0, \tag{65}$$

where the only velocity component, u, is the x-direction, and only depends on y and t.

Unidirectional motion of a viscoelastic fluid II

Eigenvalue problem

We first investigate the **relaxation behaviour of the system,** starting from a prescribed non-zero velocity field at $t = 0$ and assuming the plates remain stationary for $t > 0$. In particular we look for natural frequencies of the system that could be resonantly excited by oscillations of one plate. We seek solutions of the form

$$u(y,t) = u_\lambda(y)e^{\lambda t} + c.c. \qquad (66)$$

with $\lambda \in \mathbb{C}$, being an **eigenvalue.** Substituting (66) into (65), and considering stationary plates, we obtain

$$\rho\lambda u_\lambda - \mu^* \frac{d^2 u_\lambda}{dy^2} = 0, \qquad (67a)$$

$$u_\lambda = 0 \qquad (y = 0), \qquad (67b)$$

$$u_\lambda = 0 \qquad (y = d), \qquad (67c)$$

with

$$\mu^* = \int_0^\infty G(s)e^{-\lambda s} ds.$$

being the complex viscosity μ^* (see equation (54)). For simplicity we assume that $\mu^* = \mu' - i\mu''$ is a constant.

Unidirectional motion of a viscoelastic fluid III

We seek a solution in the form

$$u_\lambda = \sum_{m=1}^{\infty} a_m \sin\left(m\pi \frac{y}{d}\right),$$

which satisfies the boundary conditions (67b) and (67c). Substituting into (67a) we find for the m-th mode the following eigenrelationship

$$\lambda = -\frac{m^2\pi^2\mu^*}{\rho d^2}.$$

- The real part of λ is always negative and represents a decay in time of the oscillations.
- If λ is complex the system admits natural frequencies of oscillation.
- The imaginary part of λ represent the **natural frequency of the system.** It obviously depend on m, and different modes (different values of m) are associated with different natural frequencies.

Unidirectional motion of a viscoelastic fluid IV

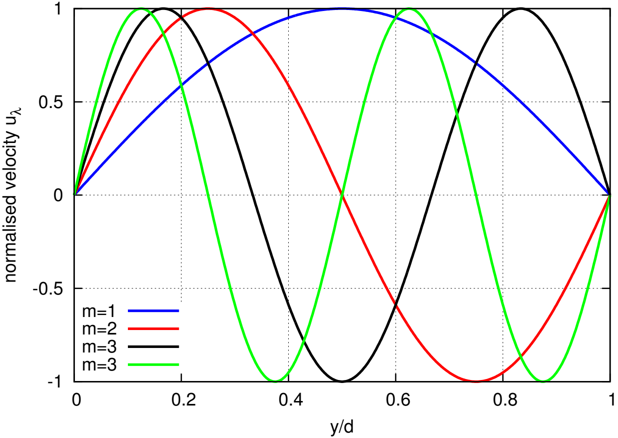

Plot of the first four eigenfunctions.

Unidirectional motion of a viscoelastic fluid V

Forced problem

We now consider the case in which the wall at $y = 0$ oscillates in the x-direction according to the following law

$$u_w = U\cos(\omega t) = \frac{U}{2}\exp(i\omega t) + c.c.,$$

where u_w is the wall velocity, U the maximum wall velocity and $c.c.$ denotes the complex conjugate.
Writing the x-component of the velocity u as $u(y,t) = \hat{u}(y)e^{i\omega t}$ the Navier–Stokes equation in the x-direction and the appropriate boundary conditions read

$$\mu^* \frac{d^2\hat{u}}{dy^2} - \rho i\omega\hat{u} = 0, \tag{68a}$$

$$\hat{u} = \frac{U}{2}, \qquad (y = 0), \tag{68b}$$

$$\hat{u} = 0, \qquad (y = d). \tag{68c}$$

The general solution of equation (68a) is

$$\hat{u} = c_1 \exp\left(\sqrt{\Gamma}y\right) + c_2 \exp\left(-\sqrt{\Gamma}y\right),$$

with $\Gamma = \rho i\omega/\mu^*$, and the constants c_1 and c_2 can be obtained by imposing the boundary conditions (68b) and (68c).

Unidirectional motion of a viscoelastic fluid VI

Velocity profiles - fixed ω and variable μ^*

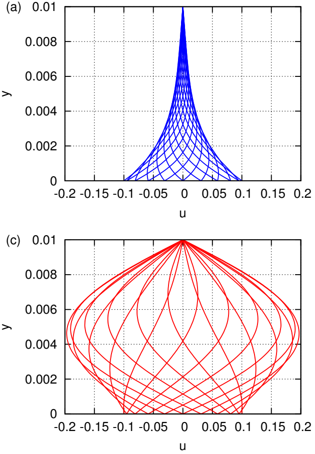

$d = 0.01$ m, $U = 0.1$ m/s, $\omega = 0.3$ rad/s. (a) $\mu^* = 0.001$ Pa·s, (b) $\mu^* = 0.001 + 0.001i$ Pa·s, (c) $\mu^* = 0.001 + 0.003i$ Pa·s **(resonance of mode $m = 1$)**, (d) $\mu^* = 0.001 + 0.005i$ Pa·s.

Unidirectional motion of a viscoelastic fluid VII

Velocity profiles - fixed μ^* and variable ω

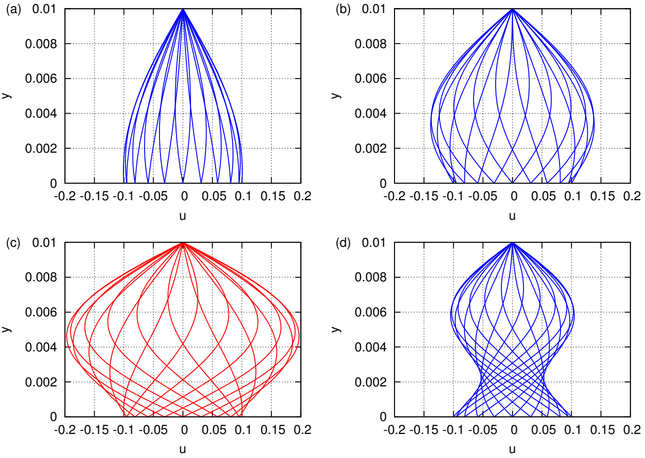

$d = 0.01$ m, $U = 0.1$ m/s, $\mu^* = 0.001 + 0.003i$ Pa·s. (a) $\omega = 0.1$ rad/s, (b) $\omega = 0.2$ rad/s, (c) $\omega = 0.3$ rad/s, **(resonance of mode $m = 1$)**, (d) $\omega = 0.5$ rad/s.

Unidirectional motion of a viscoelastic fluid VIII

Velocity profiles - excitation of different modes

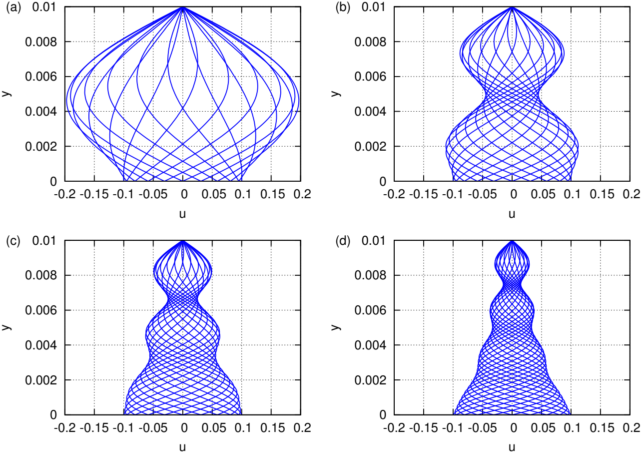

$d = 0.01$ m, $U = 0.1$ m/s, $\mu^* = 0.001 + 0.003i$ Pa·s. (a) $\omega = 0.3$ rad/s (mode $m = 1$), (b) $\omega = 1.18$ rad/s (mode $m = 2$), (c) $\omega = 2.66$ rad/s (mode $m = 3$), (d) $\omega = 4.74$ rad/s (mode $m = 4$).

Motion of a viscous fluid in a periodically rotating sphere

We now consider a more realistic problem. In particular we make the following assumptions (Repetto et al., 2005).

- **Spherical domain**
  As a first approximation we consider that the vitreous chamber has spherical shape, with radius R. The role of departure from sphericity will be discussed in the following.
  We the domain is axisymmetric we will seek **axisymmetric solutions.**
- **Purely viscous fluid**
  We first consider the case of a purely viscous, Newtonian fluid. Therefore, we should not expect the possible occurrence of resonance phenomena.
  This assumption makes sense in the following cases:
  - vitreous liquefaction;
  - substitution of the vitreous with viscous tamponade fluids, such as silicon oils.
- **Small-amplitude harmonic eye rotations**
  We assume that the sphere performs harmonic torsional oscillations with amplitude ε and frequency ω.
  The assumption of small amplitude rotations allows us to **linearise the equations.**

The mathematical details of the following analysis are not reported since they are quite technical. The student is assumed to just follow the reasoning and understand the results.

Theoretical model I

Governing equations

$$\frac{\partial}{\partial t}\mathbf{u} + (\mathbf{u}\cdot\nabla)\mathbf{u} + \frac{1}{\rho}\nabla p - \nu\nabla^2\mathbf{u} = 0,$$
$$\nabla\cdot\mathbf{u} = 0,$$
$$u = v = 0, \quad w = \varepsilon\sin\vartheta\sin t \qquad (r = R),$$

where the equations are written in terms of spherical polar coordinates (r, ϑ, φ), with r being the radial, ϑ the zenithal and φ the azimuthal coordinates. The velocity vector is written as $\mathbf{u} = (u, v, w)^T$ is the velocity vector. Moreover, ε is the amplitude of oscillations.

Solution

At leading order in an expansion in terms of the small parameter ε, it can be shown that $p = u = v = 0$ and the only component of the velocity which is non zero is $w = w(r, \vartheta)$. The solution for w is given by

$$w = -\frac{i\varepsilon\omega R^3\left(\sin\frac{ar}{R} - \frac{kr}{R}\cos\frac{ar}{R}\right)}{2r^2\left(\sin a - a\cos a\right)}e^{i\omega t}\sin\vartheta + c.c., \qquad a = e^{-i\pi/4}\alpha, \tag{69}$$

where we have defined the **Womersley number** as

$$\alpha = \sqrt{\omega R^2/\nu}.$$

Theoretical model II

Velocity profiles on the plane orthogonal to the axis of rotation at different times.

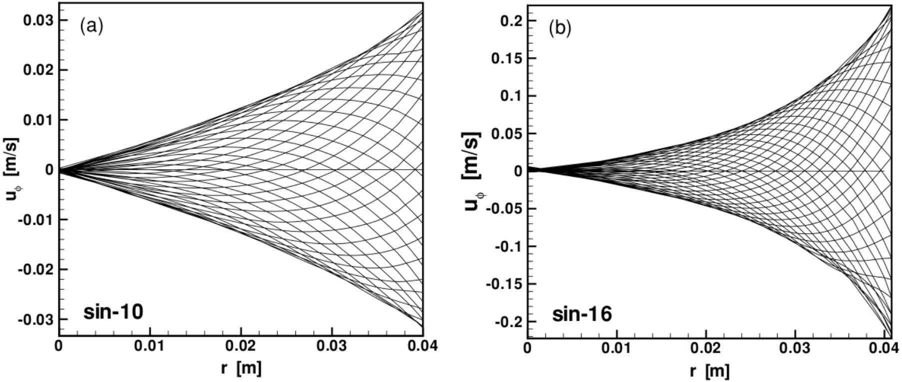

- Limit of small α: **rigid body rotation;**
- Limit of large α: formation of an **oscillatory boundary layer at the wall.**

Experimental apparatus I

- Perspex cylindrical container.
- Spherical cavity with radius $R_0 = 40$ mm.
- Glycerol (highly viscous Newtonian fluid).

Experimental apparatus II

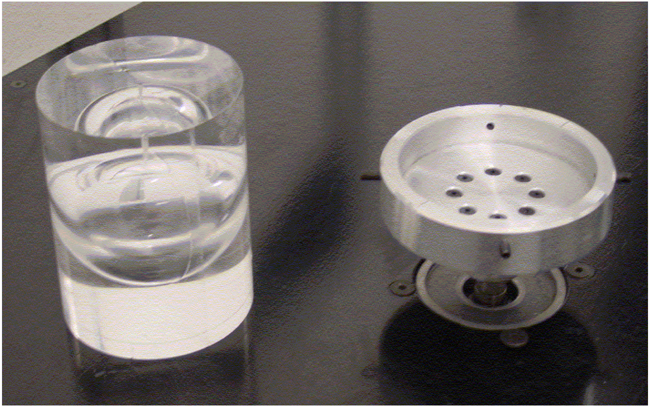

The eye model is mounted on the shaft of a computer controlled motor.

Experimental apparatus III

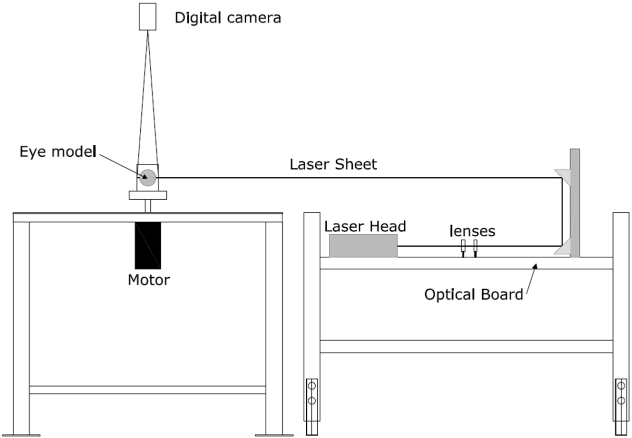

Experimental measurements I

PIV (Particle Image Velocimetry) measurements are taken on the equatorial plane orthogonal to the axis of rotation.

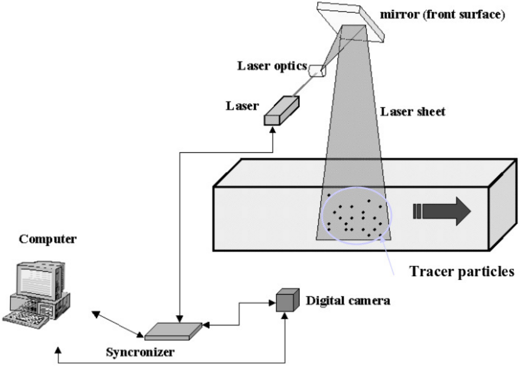

Typical PIV setup

Experimental measurements II

Typical PIV image

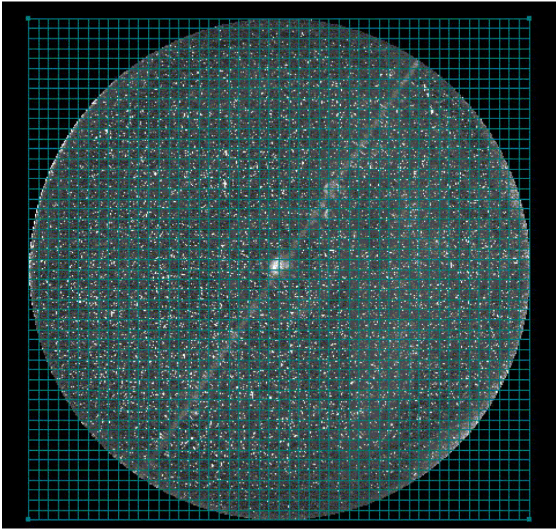

Experimental measurements III

In the PIV technique

- the image is subdivided in small **interrogation windows** (IW);
- **cross-correlation** of the image in each IW at two successive time instants yields the most likely **average displacement** $\mathbf{s}$ within the IW;
- in each IW the velocity vector is obtained as

$$\mathbf{u} = \frac{\mathbf{s}}{\Delta t},$$

with Δt time step between the two images.

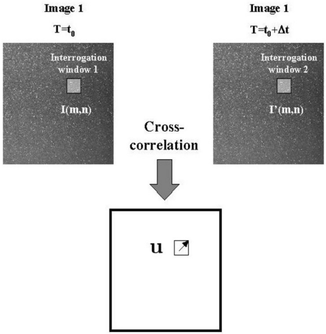

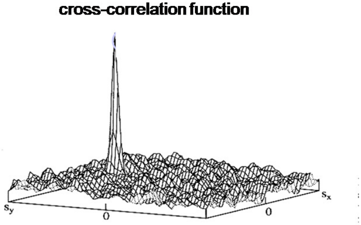

Experimental measurements IV

Typical PIV flow field

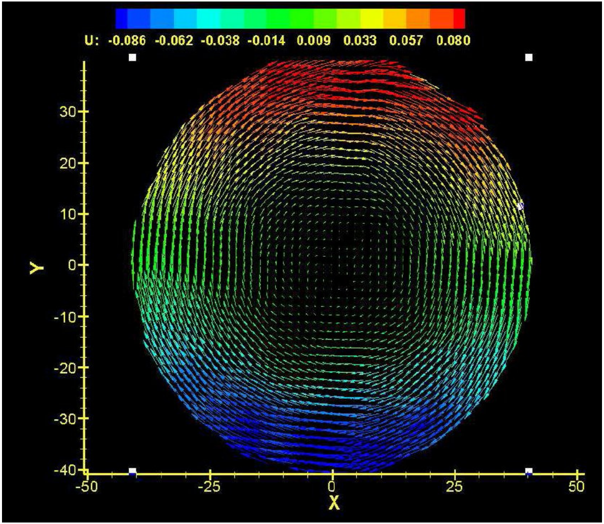

Comparison between experimental and theoretical results

Radial profiles of normalised real and imaginary parts of the velocity (see equation (69)).

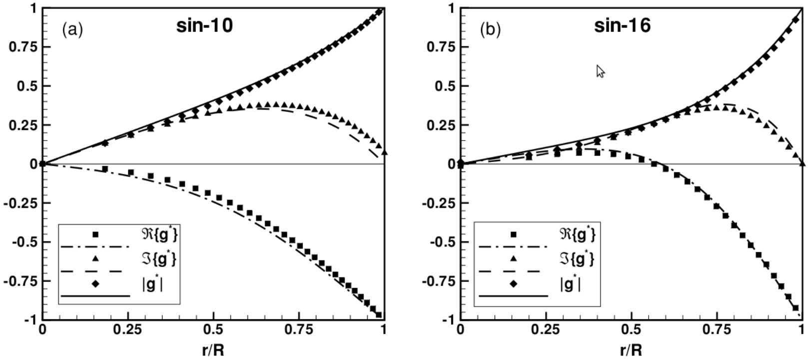

The case of a viscoelastic fluid

We now consider the case of a viscoelastic fluid within a spherical domain (Meskauskas et al., 2011).

- As we deal with an sinusoidally oscillating linear flow we can obtain the solution for the motion of a viscoelastic fluid simply by replacing the real viscosity with the **complex viscosity.**
- Rheological properties of the vitreous (complex viscosity) can be obtained from the works of Lee et al. (1992), Nickerson et al. (2008) and Swindle et al. (2008).
  Note that is this case the complex viscosity μ^* depends on the frequency of oscillations. This dependency is taken either from experimental data (where available) or is based on the use simple rheological models, such as those described at page 77.
- In this case, due to the presence of an elastic component of vitreous behaviour, the system could admit **natural frequencies** that can be excited resonantly by eye rotations.

Relaxation behaviour I

In analogy with what was shown at page 122, we seek solution with the following structure

$$\mathbf{u}(\mathbf{x}, t) = \mathbf{u}_\lambda(\mathbf{x})e^{\lambda t} + c.c., \qquad p(\mathbf{x}, t) = p_\lambda(\mathbf{x})e^{\lambda t} + c.c.,$$

where $\mathbf{u}_\lambda, p_\lambda$ do not depend on time and, in general the eigenvalue $\lambda \in \mathbb{C}$.
Substituting into the governing equations we obtain the **eigenvalue problem:**

$$\rho\lambda\mathbf{u}_\lambda = -\nabla p_\lambda + \mu^* \nabla^2 \mathbf{u}_\lambda, \qquad \nabla \cdot \mathbf{u}_\lambda = 0,$$

which has to be solved imposing **stationary no-slip conditions** at the wall and **regularity conditions** at the origin.

Relaxation behaviour II

Solution

- For all existing measurements of the rheological properties of the vitreous we find complex eigenvalues, which implies the **existence of natural frequencies of the system.**
- Such frequencies, for the least decaying modes, are within the range of physiological eye rotations ($\omega = 10 - 30$ rad/s).
- **Natural frequencies could be resonantly excited by eye rotations.**

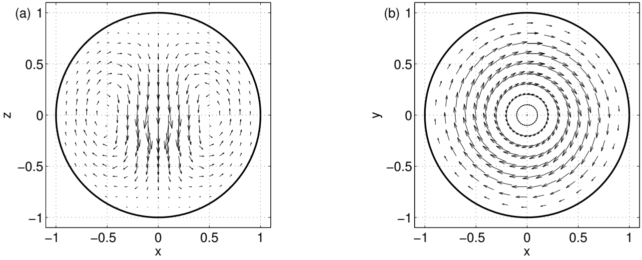

Spatial structure of two different eigenfunctions.

Periodic forcing I

We now consider the case in which the sphere performs small-amplitude harmonic torsional oscillations, with amplitude ε and frequency ω.
As in the case of Newtonian fluids **the velocity is purely azimuthal.**

Velocity profiles

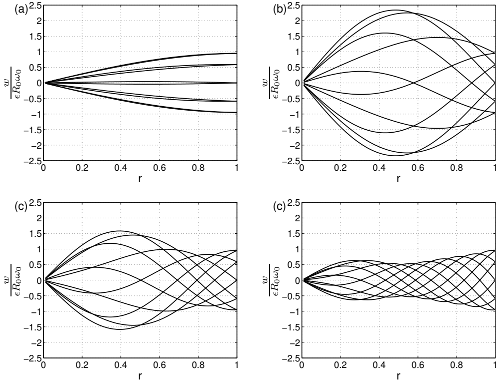

Azimuthal velocity profiles, (a) $\omega = 10$, (b) $\omega = 19.1494$, (c) $\omega = 28$, and (d) $\omega = 45$.

Periodic forcing II

Shear stress at the wall

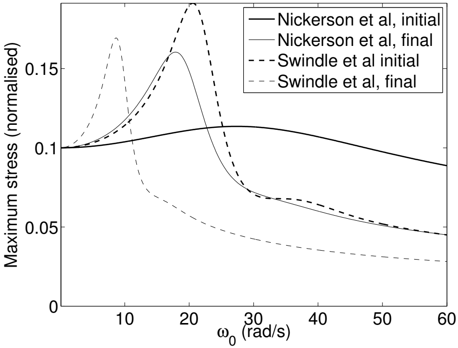

Stress normalised with $\epsilon\rho R^2\omega^2$ vs the oscillation frequency. The different curves correspond to different measurements of the vitreous rheological properties.

Some conclusions

- If the eye rotates at certain frequencies resonant excitation is possible.
- Resonance leads to large values of the stress on the retina.
- Does resonant excitation really occur in-vivo?
  - Need for in-vivo measurements of vitreous velocity (**Ultrasound scan of vitreous motion**).

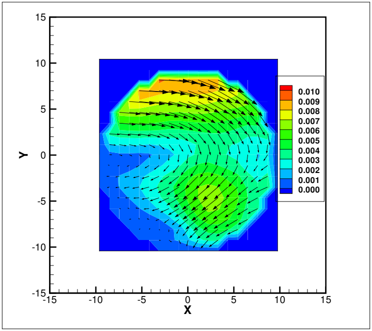

Echo-PIV measurement of vitreous motion (Rossi et al., 2012).

  - Are ex-vivo measurements of vitreous rheological properties reliable?
- The possible occurrence of resonance has implications for the choice of tamponade fluids to be used after vitrectomy.

The effect of the shape of the vitreous chamber

In reality the vitreous chamber is not exactly spherical, mainly because:

- the antero-posterior axis is shorted than the others;
- the lens produces an anterior indentation.

The non-sphericity of the domain may have an important role on the fluid dynamics in the vitreous chamber.

We consider this problem starting with a very simple **two-dimensional irrotational model.** We will then show results from three-dimensional calculations (but will not show the corresponding mathematics, which is quite technical).

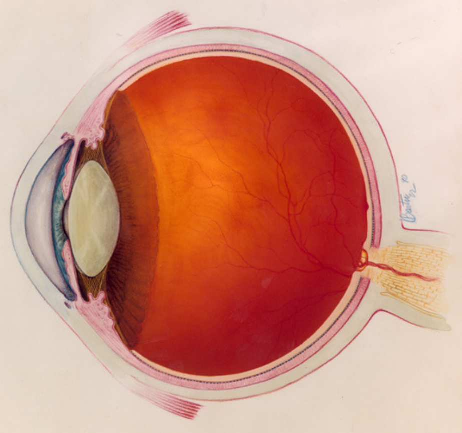

Formulation of the problem I

We consider a two-dimensional irrotational flow within a **weakly deformed, rotating circle.** Recalling the theory of irrotational flows presented at page 58, we can define a **velocity potential** Φ^* as

$$\mathbf{u}^* = \nabla \Phi^*,$$

where $\mathbf{u}^*$ denotes velocity and superscript stars indicate dimensional variables that will be made dimensionless in the following. We work in terms of polar coordinates fixed in space (r^*, ϕ), so that

$$\mathbf{u}^* = (u_r^*, u_\phi^*) = \left(\frac{\partial \Phi^*}{\partial r}, \frac{1}{r^*} \frac{\partial \Phi^*}{\partial \phi} \right). \qquad (70)$$

Fluid incompressibility implies that the velocity potential must be a harmonic function, i.e.

$$\nabla^2 \Phi^* = \frac{1}{r^*} \frac{\partial}{\partial r^*} \left(r^* \frac{\partial \Phi^*}{\partial r^*} \right) + \frac{1}{r^{*2}} \frac{\partial^2 \Phi^*}{\partial \phi^2} = 0.$$

We assume that the boundary of the domain be described by the following equation

$$F^* = r^* - R^*(\phi, t^*) = R^*[\phi - \alpha(t^*)] = 0, \qquad (71)$$

where $\alpha(t^*)$ denotes the angle of rotation of the domain with respect to a reference position. The boundary conditions impose vanishing flux through the wall. This implies

$$\frac{DF^*}{Dt^*} = \frac{\partial F^*}{\partial t^*} + \mathbf{u}^* \cdot \nabla^* F^* = 0, \qquad (F^* = 0).$$

Formulation of the problem II

Introducing (70) into the above equation and using (71) we get

$$-\frac{\partial R^*}{\partial t^*} + \frac{\partial \Phi^*}{\partial r^*} - \frac{1}{r^{*2}} \frac{\partial \Phi^*}{\partial \phi} \frac{\partial R^*}{\partial \phi} = 0 \qquad [r^* = R^*(\phi - \alpha(t^*))].$$

Once the velocity potential is known, one can compute the pressure through the Bernoulli equation (45).
Therefore, the governing equations can be written as

$$\frac{\partial}{\partial r^*}\left(r^* \frac{\partial \Phi^*}{\partial r^*}\right) + \frac{1}{r^*} \frac{\partial^2 \Phi^*}{\partial \phi^2} = 0, \tag{72a}$$

$$-\frac{\partial R^*}{\partial t^*} + \frac{\partial \Phi^*}{\partial r^*} - \frac{1}{r^{*2}} \frac{\partial \Phi^*}{\partial \phi} \frac{\partial R^*}{\partial \phi} = 0 \qquad [r^* = R^*(\phi - \alpha(t^*))] \tag{72b}$$

$$p^* = -\rho \frac{\partial \Phi^*}{\partial t^*} - \frac{1}{2}\rho \left[\left(\frac{\partial \Phi^*}{\partial r^*}\right)^2 + \frac{1}{r^{*2}}\left(\frac{\partial \Phi^*}{\partial \phi}\right)^2\right]. \tag{72c}$$

Change of coordinates I

We now perform the following change of coordinates, so that the equation of the domain becomes time independent

$$(r^*, \phi, t^*) \to (r^*, \varphi, t^*),$$

with $\varphi = \phi - \alpha(t^*)$. This implies

$$\begin{aligned}
&\frac{\partial}{\partial r^*} \to \frac{\partial}{\partial r^*},\\
&\frac{\partial}{\partial \phi} \to \frac{\partial \varphi}{\partial \phi}\frac{\partial}{\partial \varphi} = \frac{\partial}{\partial \varphi},\\
&\frac{\partial}{\partial t^*} \to \frac{\partial}{\partial t^*} + \frac{\partial \varphi}{\partial t^*}\frac{\partial}{\partial \varphi} = \frac{\partial}{\partial t} - \dot{\alpha}^*\frac{\partial}{\partial \varphi},
\end{aligned}$$

with $\dot{\alpha}^* = d\alpha/dt^*$, so that equations (72a), (72b) and (72c) become

$$\frac{\partial}{\partial r^*}\left(r^*\frac{\partial \Phi^*}{\partial r^*}\right) + \frac{1}{r^*}\frac{\partial^2 \Phi^*}{\partial \varphi^2} = 0, \tag{73a}$$

$$\dot{\alpha}^*\frac{\partial R^*}{\partial \varphi} + \frac{\partial \Phi^*}{\partial r^*} - \frac{1}{r^{*2}}\frac{\partial \Phi^*}{\partial \phi}\frac{\partial R^*}{\partial \phi} \qquad [r^* = R^*(\varphi)], \tag{73b}$$

$$p^* = \rho\dot{\alpha}^*\frac{\partial \Phi^*}{\partial \varphi} - \rho\frac{\partial \Phi^*}{\partial t^*} - \frac{1}{2}\rho\left[\left(\frac{\partial \Phi^*}{\partial r^*}\right)^2 + \frac{1}{r^{*2}}\left(\frac{\partial \Phi^*}{\partial \varphi}\right)^2\right]. \tag{73c}$$

Scaling

We scale all variables as follows

$$(r, R) = \frac{(r^*, R^*)}{\mathcal{R}}, \quad \Phi = \frac{\Phi^*}{\Omega_p \mathcal{R}^2}, \quad p = \frac{p^*}{\rho \Omega_p^2 \mathcal{R}^4}, \quad t = \Omega_p t^*, \tag{74}$$

where

- $\mathcal{R}$: radius of the circle with the same area as the actual domain;
- Ω_p: peak angular velocity of the saccadic movement.

The governing equations can be written in dimensionless form as

$$\frac{\partial}{\partial r}\left(r\frac{\partial \Phi}{\partial r}\right) + \frac{1}{r}\frac{\partial^2 \Phi}{\partial \varphi^2} = 0, \tag{75a}$$

$$\dot{\alpha}\frac{\partial R}{\partial \varphi} + \frac{\partial \Phi}{\partial r} - \frac{1}{r^2}\frac{\partial \Phi}{\partial \varphi}\frac{\partial R}{\partial \varphi} \qquad [r = R(\varphi)], \tag{75b}$$

$$p = \dot{\alpha}\frac{\partial \Phi}{\partial \varphi} - \frac{\partial \Phi}{\partial t} - \frac{1}{2}\left[\left(\frac{\partial \Phi}{\partial r}\right)^2 + \frac{1}{r^2}\left(\frac{\partial \Phi}{\partial \varphi}\right)^2\right], \tag{75c}$$

where $\dot{\alpha} = d\alpha/dt$.

Expansion

We describe the domain as a weakly deformed circle writing

$$R(\varphi) = 1 + \delta R_1(\varphi),$$

where $\delta \ll 1$ represents the maximum departure of the domain from the unit circle.

The function $R_1(\varphi)$ can be expanded in Fourier series as follows

$$R_1 = \sum_{m=1}^{\infty} a_m \cos(m\varphi) + b_m \sin(m\varphi). \tag{76}$$

Note that with the above expansion we can in principle describe any shape of the domain. Moreover, we assume that the function R_1 is symmetrical with respect to φ, and this implies $b_m = 0 \ \forall m$.

Owing to the assumption $\delta \ll 1$ we can expand Φ and p in powers of δ as follows

$$\Phi = \Phi_0 + \delta\Phi_1 + \mathcal{O}(\delta^2), \tag{77a}$$

$$p = p_0 + \delta p_1 + \mathcal{O}(\delta^2). \tag{77b}$$

Solution I

Leading order problem $\mathcal{O}(\delta^0)$

At leading order we find the trivial solution

$$\Phi_0 = 0, \qquad p_0 = \text{const}.$$

No motion is generated in a fluid within a rotating circle if the no slip condition at the wall is not imposed.

Order δ problem

At order δ the governing equations (75a)-(75c) reduce to

$$\nabla^2 \Phi_1 = 0, \tag{78a}$$

$$\frac{\partial \Phi_1}{\partial r} = -\dot{\alpha}\frac{\partial R_1}{\partial \varphi} \qquad (r = 1), \tag{78b}$$

$$p_1 = -\frac{\partial \Phi_1}{\partial t} + \dot{\alpha}\frac{\partial \Phi_1}{\partial \varphi}. \tag{78c}$$

Equation (76) and the boundary condition (78b) suggest to expand the function Φ_1 as follows

$$\Phi_1 = \sum_{m=0}^{\infty} \Phi_{1m} \sin(m\varphi).$$

Solution II

Substituting the above expansion into the equations (78a) and (78b), we obtain the following ODE

$$r\frac{d^2\Phi_{1m}}{dr^2} + \frac{d\Phi_{1m}}{dr} - \frac{m^2}{r}\Phi_{1m} = 0, \tag{79a}$$

$$\frac{d\Phi_{mn}}{dr} = ma_m\dot{\alpha} \qquad (r = 1), \tag{79b}$$

$$\text{regularity} \qquad (r = 0). \tag{79c}$$

The general solution of equation (79a) is

$$\Phi_{1m} = c_1 r^{-m} + c_2 r^m.$$

The regularity condition at the origin (79c) implies $c_1 = 0$. Imposing condition (79b) we obtain

$$\Phi_{1m} = \dot{\alpha} a_n r^{-m}. \tag{80}$$

Finally, from the linearised Bernoulli equation (78c) we find the pressure, which takes the form

$$p_1 = \sum_{m=1}^{\infty} \left[\ddot{\alpha}\sin(m\varphi) + \dot{\alpha}^2 m\cos(m\varphi)\right] a_m r^m.$$

Results I

We show here results from an analogous but three-dimensional model based on the same approach as described in the previous slides (Repetto, 2006).

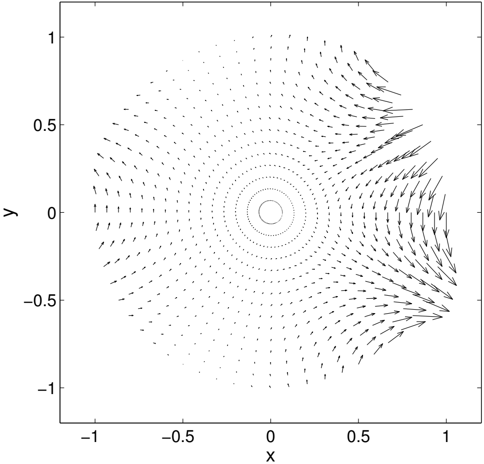

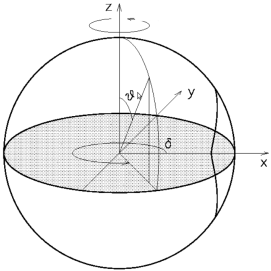

Velocity field on the equatorial plane induced by a counterclockwise rotation.

Results II

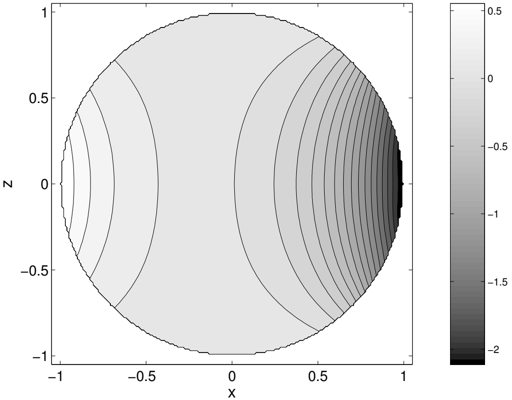

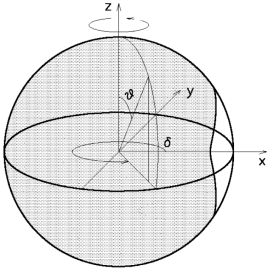

Contours of the out-of-plane velocity magnitude on the vertical plane of symmetry.

Results III

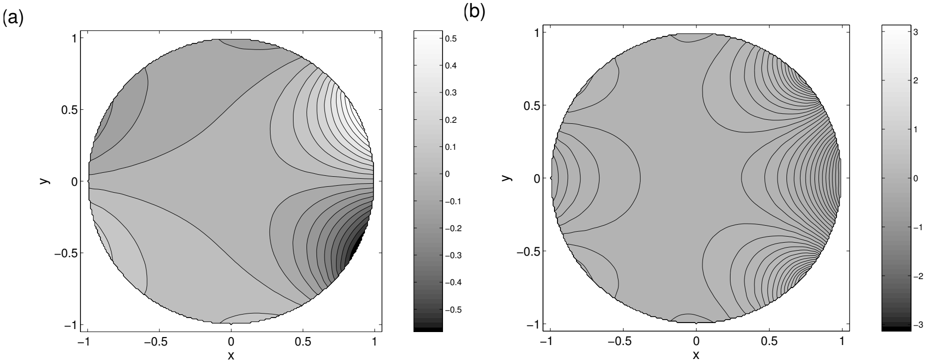

Pressure field on the equatorial plane.

- (a) time of maximum angular acceleration.
- (b) time of maximum angular velocity.

Some conclusions

- This simple model suggests that, especially in the case of low viscosity fluids, **the shape of the vitreous chamber plays a significant role in vitreous motion.**
- The flow field is complex and significantly three-dimensional.
- A circulation is likely to form in the anterior part on the vitreous chamber, close to the lens.

Vitreous motion in myopic eyes

The approach adopted in the previous section to treat the non-sphericity of the domain can also be employed to study the **motion of a viscoelastic fluid in a quasi-spherical domain.**
We describe here the particular case of **myopic eyes** (Meskauskas et al., 2012).
In comparison to emmetropic eyes, myopic eyes are

- larger in all directions;
- particularly so in the antero-posterior direction.

Myopic eyes bear **higher risks of posterior vitreous detachment and vitreous degeneration** and, consequently, an **increased the risk of rhegmatogeneous retinal detachment.**

The shape of the eye ball has been related to the degree of myopia (measured in dioptres D) by Atchison et al. (2005), who approximated the vitreous chamber with an ellipsoid.

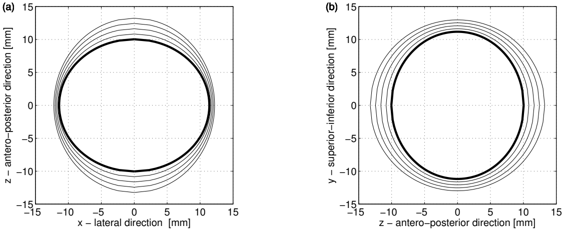

(a) horizontal and (b) vertical cross sections of the domain for different degrees of myopia.

Mathematical problem

Equation of the boundary

We again describe the domain as a weakly deformed sphere, writing

$$R(\vartheta, \varphi) = \mathcal{R}(1 + \delta R_1(\vartheta, \varphi)),$$

where

- $\mathcal{R}$ denotes the radius of the sphere with the same volume as the vitreous chamber;
- δ is a **small parameter** ($\delta \ll 1$);
- the maximum absolute value of R_1 is 1.

Expansion

We expand the velocity and pressure fields in terms of δ as follows

$$\mathbf{u} = \mathbf{u}_0 + \delta \mathbf{u}_1 + \mathcal{O}\left(\delta^2\right), \qquad p = p_0 + \delta p_1 + \mathcal{O}\left(\delta^2\right).$$

Leading order problem $\mathcal{O}(\delta^0)$

At leading order we find the solution in a sphere, discussed at page 146.

Order δ problem

The solution at order δ can be found in the form of a series expansion, similarly to what was done in the case of the irrotational model (see page 140).

Solution I

Stress distribution on the retina

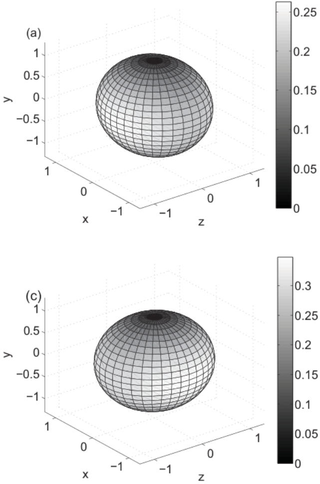

Spatial distribution of (a, c) the maximum dimensionless tangential stress and (b, d) normal stress. (a) and (b): emmetropic eye; (c) and (d): myopic eye with refractive error 20 D.

Solution II

Maximum stress on the retina as a function of the refractive error

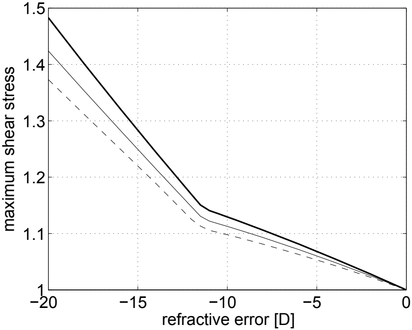

Maximum (over time and space) of the tangential tress on the retina as a function of the refractive error in dioptres. Values are normalised with the corresponding stress in the emmetropic (0 D) eye. The different curves correspond to different values of the rheological properties of the vitreous humour taken from the literature.

Some conclusions

- The vitreous and the retina in myopic eyes are continuously subjected to **significantly higher shear stresses than emmetropic eyes.**
- This provides a feasible explanation for why in myopic eyes vitreous liquefaction, posterior vitreous detachment and retinal detachment are more frequent than in emmetropic eyes.

Flow in axons of the optic nerve during glaucoma

Introduction I

The optic nerve

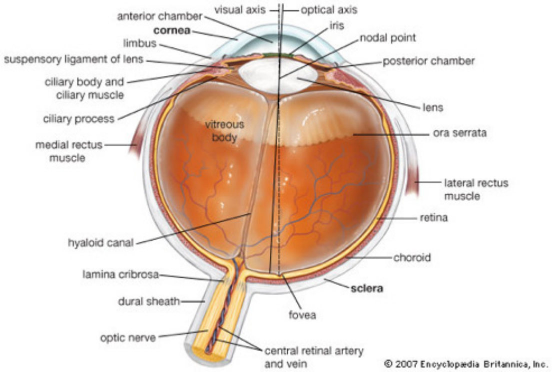

- The optic nerve acts like a cable connecting the eye with the brain.
- It transmits electrical impulses from the retina to the brain.
- It connects to the back of the eye near the macula.

Introduction II

Neuronal connectivity of the retina

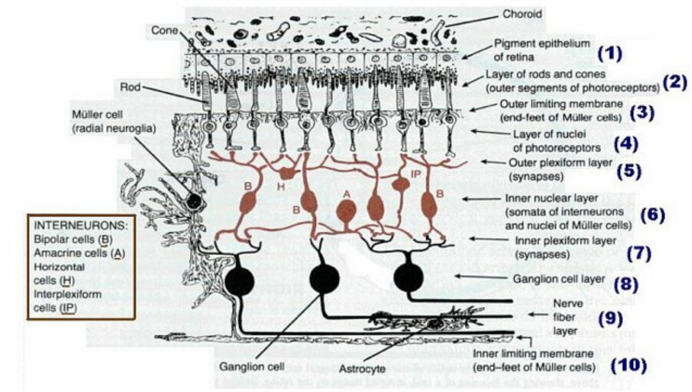

- The axons in the retina are about **15 cm long.**
- They pass **from the retina** through the optic nerve head along the optic nerve and **into the brain.**
- There are approximately **one million** retinal ganglion cells (and therefore one million axons!

Introduction III

The optic nerve head

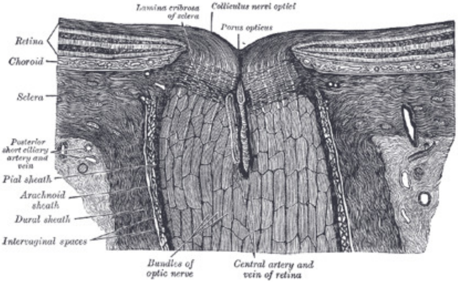

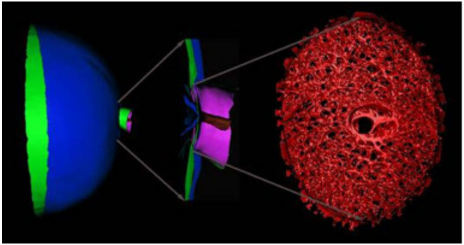

Section of the optic nerve head and the lamina cribrosa.

Introduction IV

The lamina cribrosa

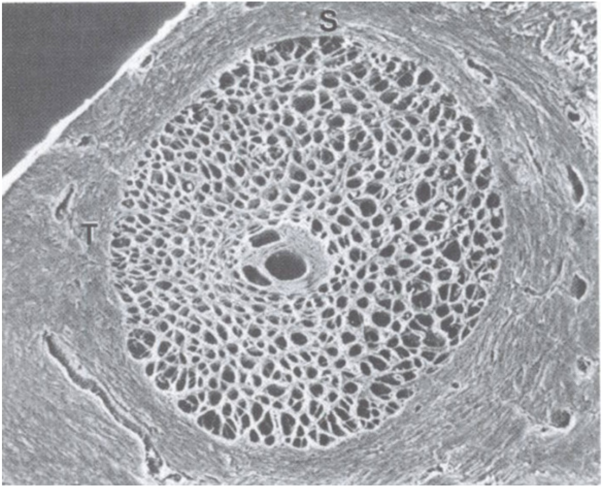

Lamina cribrosa.

Glaucoma

- Glaucoma is a disease of the eye that gradually narrows the field of vision.
- This progression of damage can culminate in total blindness.
- Glaucoma is the second leading cause of blindness worldwide.

Normal vision

Same scene as viewed by a person with glaucoma

- It causes the progressive loss of **retinal ganglion cells**, giving rise to an **optic neuropathy**.
- The mechanisms that initiate and fuel progression of the disease are not well understood. However, it is known that **glaucoma is related to high intraocular pressure**.

Possible mechanisms causing glaucoma

The mechanism whereby a high intraocular pressure leads to the loss of retinal ganglion cells has so far proven to be enigmatic.

There are two main theories:

- Cell loss due to mechanical deformation (e.g. Yan et al., 1994; Burgoyne et al., 2005).
- Adverse effect on vascular perfusion (e.g. Yamamoto and Kitazawa, 1998).

Theory of mechanical deformation I

Basic assumption:

- An **increase in IOP induces mechanical stress** in the load-bearing tissues of the optic-nerve (the lamina cribrosa, peripapillary sclera and scleral canal), which **causes tissue deformation**.
- As the tissue deforms, it pinches the retinal ganglion cells inducing **physiological stress that could lead to cell death**.
- **Several FEM models** have been developed to understand the impact of a raised intraocular pressure on the biomechanics of the optic-nerve head (e.g. Sigal et al., 2004, 2005).

Theory of mechanical deformation II

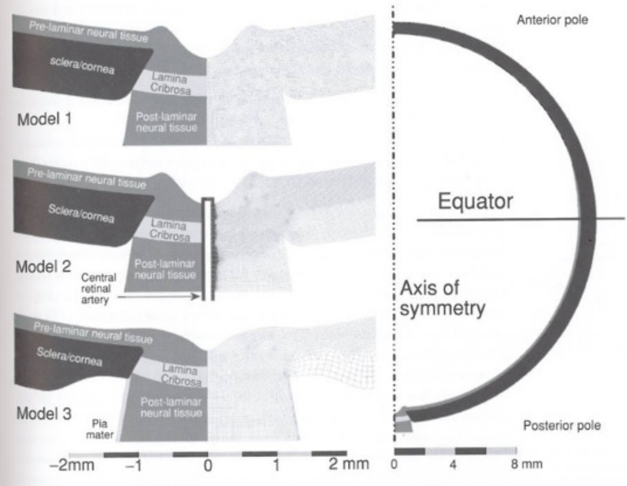

From Ethier and Simmons (2007).

Theory of vascular perfusion

Basic assumption:

- The intraocular circulation is **autoregulated**. We know this because **tissue perfusion is independent of pressure**.
- It is hypothesised that glaucoma induces **faulty autoregulation of blood flow** in the optic-nerve head (e.g. Evans et al., 1999; Flammer et al., 2002).
- However, a modest elevation of intraocular pressure, in the region of 10 mm Hg, can lead to optic neuropathy, even though this elevation is well within the range in which autoregulation will operate.

Facts about the functions of neurons

Basic assumptions

- **Active axonal transport (AAT):** this transports necessary substances in vesicles along the axons,
- AAT is induced by motor molecules:
  - **dynein** (retrograde transport: synapse to cell body),
  - **kinesin** (orthograde transport: cell body to synapse).
- Dynein and kinesin **gain energy by ATP** (adesosine triphosphate),
- ATP is **distributed throughout the axons primarily by diffusion**.

A possible alternative mechanism for glaucoma generation I

Band et al. (2009)

Hypothesised sequence of events

- The **difference between** the intraocular and cerebro-spinal **pressures causes fluid flow** along the axons, called **P**assive **N**euronal **I**ntracellular **F**luid **F**low (**PNIFF**).
- The **PNIFF disrupts the diffusive transport** of ATP and creates a 'wash out' zone close to the lamina cribrosa in which **ATP is depleted**.
- The ATP depletion **leads to an energy deficiency** that disrupts AAT. The axons will then not be able to maintain communication between the cell body and the synapse, which could **lead to cell death**.

A possible alternative mechanism for glaucoma generation II

The mathematical model

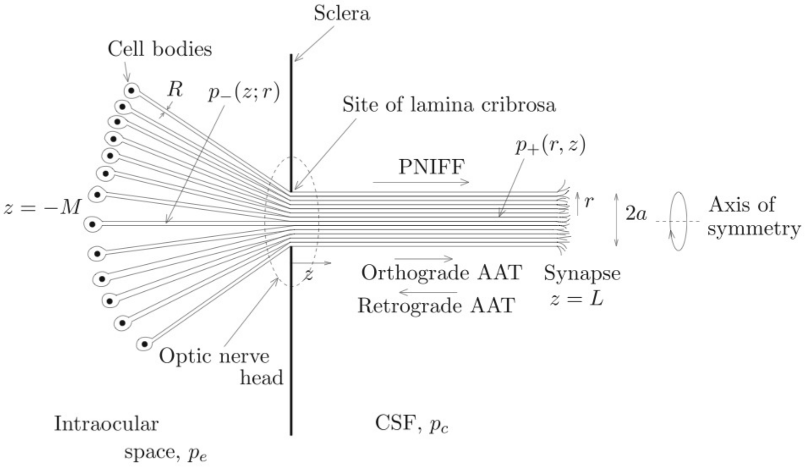

1D model **2D model**

Typical values of the parameters

Parameter		Value	Ref.
R	Axon radius	$13.5 \times 10^{-6}\,\mathrm{m}$	●
a	Optic-nerve radius	$7.5 \times 10^{-4}\,\mathrm{m}$	●
μ	Axoplasm viscosity	$0.01\,\mathrm{Pa\,s}$	●
κ_-	Axon membrane conductivity in the eye	$10^{-11}\mathrm{m\,s^{-1}\,Pa^{-1}}$	●
κ_+	Axon membrane conductivity in the optic nerve	$10^{-12}\mathrm{m\,s^{-1}\,Pa^{-1}}$	●
p_e	Intraocular pressure (30 mmHg)	$4.0 \times 10^{3}\,\mathrm{Pa}$	●
p_c	CSF pressure (10 mmHg)	$1.3 \times 10^{3}\,\mathrm{Pa}$	●
M	Length of axon in the eye	$0.01\,\mathrm{m}$	●
L	Length of axon in the optic nerve	$0.10\,\mathrm{m}$	●
l	Diffusive length scale for ATP	$10^{-5}\,\mathrm{m}$	●
D	Diffusion coefficient for ATP	$3 \times 10^{-10}\,\mathrm{m^2\,s^{-1}}$	●

- **Reliable data from the literature**
- **No data from the literature**
- **Very sparse or uncertain data**

Formulation of the mathematical problem I

Flow in the axons

Model using **Poiseuille flow**

$$\text{Flux} \qquad F(r,z) = -\frac{\pi R^4}{8\mu}\frac{\partial p}{\partial z}, \tag{81}$$

$$\text{Velocity} \quad U(r,z) = \frac{2F}{\pi R^2} = \frac{R^2}{4\mu}\frac{\partial p}{\partial z}. \tag{82}$$

Problem in the eye (1D model, $z < 0$)

$$-\frac{d}{dz}\left(\frac{\pi R^4}{8\mu}\frac{dp_-}{dz}\right) + \underbrace{2\pi R \kappa_- \left(p_- - p_e\right)}_{\text{flux through wall}} = 0. \tag{83}$$

Formulation of the mathematical problem II

Problem in the optic nerve (2D model, $z > 0$)

- The cross-section of the optic nerve is approximated as a hexagonal lattice of axons.
- Each axon is labelled by the (x, y) coordinate of its centre.
- The pressure in a given axon only depends on z, thus $p_{(x_0,y_0)}(z)$ denotes the value of p_+ in the axon centred on (x_0, y_0).

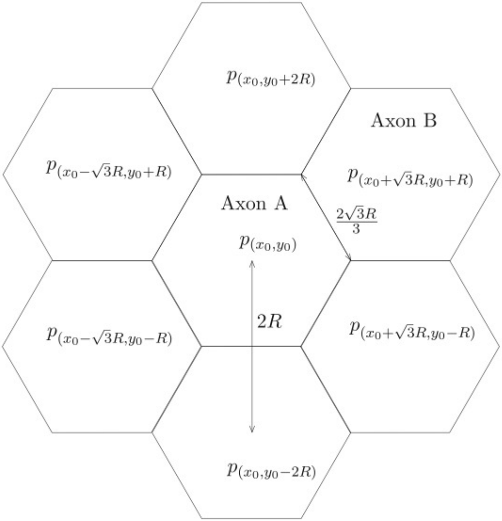

Formulation of the mathematical problem III

Flux per unit area across the axon's membrane (*e.g*, A → B)

$$F_{AB} = -\frac{R\kappa_+}{\sqrt{3}}\left(p_{(x_0+\sqrt{3}R,y_0+R)} - p_{(x_0,y_0)}\right). \quad (84)$$

Since $R \ll a$, a Taylor series can be used to approximate these discrete pressure differences by continuous pressure differences:

$$F_{AB} = -\frac{R\kappa_+}{\sqrt{3}}\left(\sqrt{3}R\frac{\partial p_+}{\partial x} + R\frac{\partial p_+}{\partial y} + \frac{3R^2}{2}\frac{\partial^2 p_+}{\partial x^2} + \sqrt{3}R^2\frac{\partial^2 p_+}{\partial x \partial y} + \frac{R^2}{2}\frac{\partial^2 p_+}{\partial y^2}\right). \quad (85)$$

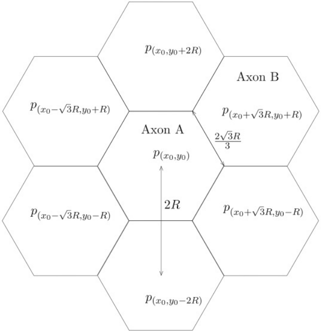

Formulation of the mathematical problem IV

Summing over the six edges of the axon A:

$$\frac{\partial F}{\partial z} = \frac{R\kappa_+}{\sqrt{3}} \Big(p_{(x_0,y_0+2R)} + p_{(x_0+\sqrt{3}R,y_0+R)} + p_{(x_0-\sqrt{3}R,y_0+R)}$$
$$+ p_{(x_0+\sqrt{3}R,y_0-R)} + p_{(x_0-\sqrt{3}R,y_0-R)} + p_{(x_0,y_0-2R)} - 6p_{(x_0,y_0)} \Big), \quad (86)$$

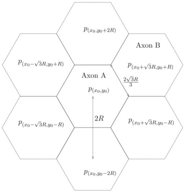

and, using a Taylor series to approximate the above expression:

$$\frac{\partial F}{\partial z} \approx 2\sqrt{3}R^3\kappa_+ \left(\frac{\partial^2 p_+}{\partial x^2} + \frac{\partial^2 p_+}{\partial y^2} \right) = \frac{2\sqrt{3}R^3\kappa_+}{r} \frac{\partial}{\partial r}\left(r \frac{\partial p_+}{\partial r} \right). \quad (87)$$

Introduce Poiseuille's law to evaluate F:

$$-\frac{\partial}{\partial z}\left(\frac{\sqrt{3}R^4}{4\mu} \frac{\partial p_+}{\partial z} \right) - \frac{2\sqrt{3}R^3\kappa_+}{r} \frac{\partial}{\partial r}\left(r \frac{\partial p_+}{\partial r} \right) = 0 \quad \text{for } 0 < r < a,\ z > 0. \quad (88)$$

Formulation of the mathematical problem V

Boundary conditions:

- **Regularity at the centre and continuity of pressure at the edge of the optic nerve:**

$$\frac{\partial p_+}{\partial r} = 0 \text{ on } r = 0, \quad p_+ = p_c \text{ on } r = a, \tag{89}$$

  where p_c is the pressure of the cerebro-spinal fluid.

- No flux through the ends of the axons:

$$F = 0 \quad \text{at } z = L, -M. \tag{90}$$

- Continuity of the pressure and flux across the lamina cribrosa

$$p_- = p_+ \quad \frac{dp_-}{dz} = \frac{\partial p_+}{\partial z} \quad \text{at } z = 0. \tag{91}$$

Solution I

Nondimensionalisation

$$p_\pm = p_c + (p_e - p_c)\,\hat{p}_\pm, \quad r = a\hat{r}, \quad z = L\hat{z}, \tag{92}$$

Dimensionless parameters

$$m = \frac{M}{L}, \quad l_o = \frac{1}{L}\sqrt{\frac{Ra^2}{8\mu\kappa_+}}, \quad l_e = \frac{1}{M}\sqrt{\frac{R^3}{16\mu\kappa_-}}, \tag{93}$$

so that

- m is the ratio of the length of the axon in the eye and the length in the optic nerve,
- l_o is the ratio of the axial length scale over which the flux across the axons' membranes influences the axoplasmic pressure in the optic nerve and the length of the optic nerve, and
- l_e is the ratio of the axial length scale over which the flux across the axons' membranes influences the axoplasmic pressure in the eye and the length of the axon in the eye.

Solution II

Dimensionless equations and boundary conditions

$$l_o^2 \frac{\partial^2 p_+}{\partial z^2} + \frac{1}{r}\frac{\partial}{\partial r}\left(r \frac{\partial p_+}{\partial r} \right) = 0 \quad \text{in } z > 0 \qquad \text{problem in the optic nerve} \qquad (94)$$

$$-m^2 l_e^2 \frac{d^2 p_-}{dz^2} + p_- - 1 = 0 \quad \text{in } z < 0 \qquad \text{problem in the eye} \qquad (95)$$

$$\left.\begin{array}{ll} \dfrac{\partial p_+}{\partial r} = 0 & \text{at } r = 0 \\ p_+ = 0 & \text{at } r = 1 \\ \frac{dp_-}{dz} = 0 & \text{at } z = -m \\ \dfrac{\partial p_+}{\partial z} = 0 & \text{at } z = 1 \\ \left.\begin{array}{c} p_- = p_+ \\ \frac{dp_-}{dz} = \dfrac{\partial p_+}{\partial z} = 0 \end{array}\right\} & \text{at } z = 0 \end{array}\right\} \qquad \text{boundary conditions} \qquad (96)$$

Solution III

Solution in the eye

$$p_-(z;r) = 1 + A(r)\left(e^{z/(l_e m)} + e^{-(2m+z)/(l_e m)}\right), \qquad (97)$$

for $z < 0$ (we have applied the boundary condition at $z = -m$.

Solution IV

Solution in the optic nerve

Use separation of variables to obtain the general solution for p_+ as a sum of functions of the form

$$\left(C^{(1)}e^{\lambda z/l_o}+C^{(2)}e^{-\lambda z/l_o}\right)\left(C^{(3)}J_0(\lambda r)+C^{(4)}Y_0(\lambda r)\right), \tag{98}$$

where J_0 and Y_0 are Bessel functions of the first and second kinds respectively at order zero.
Apply the boundary conditions to obtain $C^{(4)}=0$ and $e^{2\lambda_j/l_o}C_j^{(1)}=C_j^{(2)}$, and hence

$$p_+\left(r,z\right)=\sum_{j=1}^{\infty}C_j\left(e^{\lambda_j z/l_o}+e^{\lambda_j(2-z)/l_o}\right)J_0\left(\lambda_j r\right), \tag{99}$$

where

$$C_j=\left(1-e^{-2/l_e}\right)\frac{1}{\lambda_j}J_1(\lambda_j)\left(\int_0^1 r\left(J_0(\lambda_j r)\right)^2 dr\right)^{-1}$$
$$\times\left[\left(1+e^{2\lambda_j/l_o}\right)\left(1-e^{-2/l_e}\right)-\frac{ml_e\lambda_j}{l_o}\left(1+e^{-2/l_e}\right)\left(1-e^{2\lambda_j/l_o}\right)\right]^{-1}, \tag{100}$$

$$A(r)=\left(-1+\sum_{j=1}^{\infty}C_j\left(1+e^{2\lambda_j/l_o}\right)J_0(\lambda_j r)\right)\left(1+e^{-2/l_e}\right)^{-1}. \tag{101}$$

Results I

Axoplasmic pressure and flux close to the edge of the optic nerve

For IOP = 30 mmHg

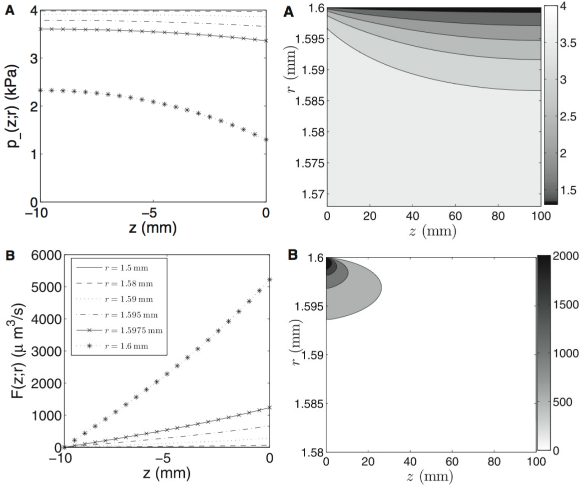

Results II

- In health ATP is distributed along the axon primarily by diffusion.
- The PNIFF is expected to influence the ATP distribution by advecting ATP downstream.
- This may result in depletion of ATP locally.

The relative importance of advection to diffusion is characterised by the **Peclet number**

$$Pe = Ul/D \tag{102}$$

Large Pe: advection dominates
Small Pe: diffusion dominates

where

U	characteristic velocity
l	characteristic lengthscale of the diffusion process
D	diffusion coefficient

Note: Since ATP is produced by mitochondria it must diffuse between them to supply energy throughout the axon. Therefore we could base our estimate of the lengthscale l on the average distance between neighbouring mitochondria.

Results III

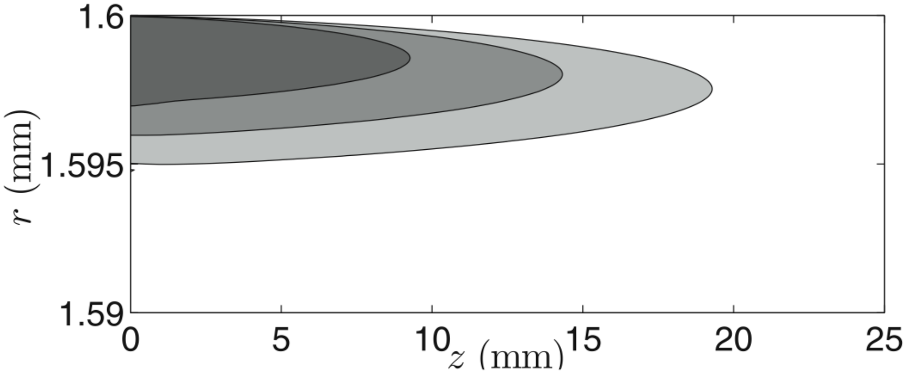

Damage is expected to occur in regions where *Pe* is order 1 or larger. **The shaded parts of this figure show the regions where $Pe > 1$ for three different IOP's.** These are the regions in which the model predicts that damage could occur.

Conclusions

- The mathematical model shows that the PNIFF mechanism is a plausible explanation for the generation of glaucoma.
- Although the PNIFF may transport material to compensate the breakdown of orthograde AAT, the retrograde transport would still be impaired.
- Both orthograde and retrograde transports are essential for cell functionality.
- The locations of reduced AAT are qualitatively consistent with experimental observations.
- This model does not exclude the possibility that other mechanisms (*e.g.* mechanical deformation of the lamina cribrosa) may also contribute to cell death in the optic nerve.
- Accounting for the finite thickness of the lamina cribrosa made relatively little difference to the results.

Important note

- The PNIFF mechanism presented here predicts that it is the pressure difference between the IOP and the pressure in the cerebro-spinal fluid that induces AAT disruption, as opposed to the absolute value of the IOP.
- Low pressures in the cerebro-spinal fluid have recently been observed in patients with glaucoma.

Appendix: the equations of motion in different coordinates systems

Cylindrical coordinates

Let us consider cylindrical coordinates (z, r, φ), with corresponding velocity components (u_z, u_r, u_φ).

Continuity equation

$$\frac{\partial u_z}{\partial z} + \frac{1}{r}\frac{\partial}{\partial r}(r u_r) + \frac{1}{r}\frac{\partial u_\varphi}{\partial \varphi} = 0 \tag{103}$$

Navier-Stokes equations

$$\frac{\partial u_z}{\partial t} + u_z \frac{\partial u_z}{\partial z} + u_r \frac{\partial u_z}{\partial r} + \frac{u_\varphi}{r}\frac{\partial u_z}{\partial \varphi} + \frac{1}{\rho}\frac{\partial p}{\partial z} - \nu \left[\frac{\partial^2 u_z}{\partial z^2} + \frac{1}{r}\frac{\partial}{\partial r}\left(r \frac{\partial u_z}{\partial r} \right) + \frac{1}{r^2}\frac{\partial^2 u_z}{\partial \varphi^2} \right] = 0. \tag{104}$$

$$\frac{\partial u_r}{\partial t} + u_z \frac{\partial u_r}{\partial z} + u_r \frac{\partial u_r}{\partial r} + \frac{u_\varphi}{r}\frac{\partial u_r}{\partial \varphi} - \frac{u_\varphi^2}{r} + \frac{1}{\rho}\frac{\partial p}{\partial r} +$$
$$- \nu \left[\frac{\partial^2 u_r}{\partial z^2} + \frac{1}{r}\frac{\partial}{\partial r}\left(r \frac{\partial u_r}{\partial r} \right) + \frac{1}{r^2}\frac{\partial^2 u_r}{\partial \varphi^2} - \frac{u_r}{r^2} - \frac{2}{r^2}\frac{\partial u_\varphi}{\partial \varphi} \right] = 0. \tag{105}$$

$$\frac{\partial u_\varphi}{\partial t} + u_z \frac{\partial u_\varphi}{\partial z} + u_r \frac{\partial u_\varphi}{\partial r} + \frac{u_\varphi}{r}\frac{\partial u_\varphi}{\partial \varphi} + \frac{u_r u_\varphi}{r} + \frac{1}{\rho r}\frac{\partial p}{\partial \varphi} +$$
$$- \nu \left[\frac{\partial^2 u_\varphi}{\partial z^2} + \frac{1}{r}\frac{\partial}{\partial r}\left(r \frac{\partial u_\varphi}{\partial r} \right) + \frac{1}{r^2}\frac{\partial^2 u_\varphi}{\partial \varphi^2} + \frac{2}{r^2}\frac{\partial u_r}{\partial \varphi} - \frac{u_\varphi}{r^2} \right] = 0. \tag{106}$$

Spherical polar coordinates I

Let us consider spherical polar coordinates (r, ϑ, φ) (radial, zenithal and azimuthal), with corresponding velocity components $(u_r, u_\vartheta, u_\varphi)$.

Continuity equation

$$\frac{1}{r^2}\frac{\partial}{\partial r}\left(r^2 u_r\right) + \frac{1}{r\sin\vartheta}\frac{\partial}{\partial\vartheta}\left(\sin\vartheta u_\vartheta\right) + \frac{1}{r\sin\vartheta}\frac{\partial u_\varphi}{\partial\varphi} = 0. \tag{107}$$

Navier-Stokes equations

$$\begin{aligned}
&\frac{\partial u_r}{\partial t} + u_r\frac{\partial u_r}{\partial r} + \frac{u_\vartheta}{r}\frac{\partial u_r}{\partial\vartheta} + \frac{u_\varphi}{r\sin\vartheta}\frac{\partial u_r}{\partial\varphi} - \frac{u_\vartheta^2}{r} - \frac{u_\varphi^2}{r} + \frac{1}{\rho}\frac{\partial p}{\partial r} + \\
&\quad - \nu\left[\frac{1}{r^2}\frac{\partial}{\partial r}\left(r^2\frac{\partial u_r}{\partial r}\right) + \frac{1}{r^2\sin\vartheta}\frac{\partial}{\partial\vartheta}\left(\sin\vartheta\frac{\partial u_r}{\partial\vartheta}\right) + \frac{1}{r^2\sin^2\vartheta}\frac{\partial^2 u_r}{\partial\varphi^2} + \right.\\
&\quad\left. - \frac{2u_r}{r^2} - \frac{2}{r^2\sin\vartheta}\frac{\partial(u_\vartheta\sin\vartheta)}{\partial\vartheta} - \frac{2}{r^2\sin\vartheta}\frac{\partial u_\varphi)}{\partial\varphi}\right] = 0.
\end{aligned} \tag{108}$$

$$\begin{aligned}
&\frac{\partial u_\vartheta}{\partial t} + u_r\frac{\partial u_\vartheta}{\partial r} + \frac{u_\vartheta}{r}\frac{\partial u_\vartheta}{\partial\vartheta} + \frac{u_\varphi}{r\sin\vartheta}\frac{\partial u_\vartheta}{\partial\varphi} + \frac{u_r u_\vartheta}{r} - \frac{u_\varphi^2\cot\vartheta}{r} + \frac{1}{\rho r}\frac{\partial p}{\partial\vartheta} + \\
&\quad - \nu\left[\frac{1}{r^2}\frac{\partial}{\partial r}\left(r^2\frac{\partial u_\vartheta}{\partial r}\right) + \frac{1}{r^2\sin\vartheta}\frac{\partial}{\partial\vartheta}\left(\sin\vartheta\frac{\partial u_\vartheta}{\partial\vartheta}\right) + \frac{1}{r^2\sin^2\vartheta}\frac{\partial^2 u_\vartheta}{\partial\varphi^2} + \right.
\end{aligned}$$

Spherical polar coordinates II

$$+\frac{2}{r^2}\frac{\partial u_r}{\partial \vartheta} - \frac{u_\vartheta}{r^2 \sin^2 \vartheta} - \frac{2\cos\vartheta}{r^2 \sin^2\vartheta}\frac{\partial u_\varphi)}{\partial \varphi}\bigg] = 0. \quad (109)$$

$$\frac{\partial u_\varphi}{\partial t} + u_r \frac{\partial u_\varphi}{\partial r} + \frac{u_\vartheta}{r}\frac{\partial u_\varphi}{\partial \vartheta} + \frac{u_\varphi}{r \sin\vartheta}\frac{\partial u_\varphi}{\partial \varphi} + \frac{u_r u_\varphi}{r} + \frac{u_\vartheta u_\varphi \cot\vartheta}{r} + \frac{1}{\rho r \sin\vartheta}\frac{\partial p}{\partial \varphi} +$$

$$-\nu\left[\frac{1}{r^2}\frac{\partial}{\partial r}\left(r^2 \frac{\partial u_\varphi}{\partial r}\right) + \frac{1}{r^2 \sin\vartheta}\frac{\partial}{\partial \vartheta}\left(\sin\vartheta \frac{\partial u_\varphi}{\partial \vartheta}\right) + \frac{1}{r^2\sin^2\vartheta}\frac{\partial^2 u_\varphi}{\partial \varphi^2} + \right.$$

$$\left. + \frac{2}{r^2 \sin\vartheta}\frac{\partial u_r}{\partial \varphi} + \frac{2\cos\vartheta}{r^2\sin^2\vartheta}\frac{\partial u_\vartheta}{\partial \varphi} - \frac{u_\varphi}{r^2 \sin^2\vartheta}\right] = 0. \quad (110)$$

References I

D. A. Atchison, N. Pritchard, K. L. Schmid, D. H. Scott, C. E. Jones, and J. M. Pope. Shape of the retinal surface in emmetropia and myopia. *Investigative Ophthalmology & Visual Science*, 46(8):2698–2707, 2005. doi: 10.1167/iovs.04-1506.

L. R. Band, C. L. Hall, G. Richardson, O. E. Jensen, J. H. Siggers, and A. J. E. Foss. Intracellular flow in optic nerve axons: A mechanism for cell death in glaucoma. *Investigative Ophthalmology & Visual Science*, 50(8):3750 –3758, 2009. doi: 10.1167/iovs.08-2396.

W. Becker. Metrics. In R. Wurtz and M. Goldberg, editors, *The neurobiology of saccadic eye movements*. Elsevier Science Publisher BV (Biomedical Division), 1989.

R. J. Braun. Dynamics of the tear film. *Annual Review of Fluid Mechanics*, 44(1):267–297, 2012. doi: 10.1146/annurev-fluid-120710-101042.

C. Burgoyne, J. Downs, A. Bellezza, J. Suh, and R. Hart. The optic nerve head as a biomechanical structure: a new paradigm for understanding the role of iop-related stress and strain in the pathophysiology of glaucomatous optic nerve head damage. *Prog. Retin. Eye Res.*, 24:39–73, 2005.

C. R. Canning, M. J. Greaney, J. N. Dewynne, and A. Fitt. Fluid flow in the anterior chamber of a human eye. *IMA Journal of Mathematics Applied in Medicine and Biology*, 19:31–60, 2002.

C. R. Ethier and C. A. Simmons. *Introductory Biomechanics - From Cells to Organisms*. (Cambridge Texts in Biomedical Engineering) Cambridge University Press, 2007.

C. R. Ethier, M. Johnson, and J. Ruberti. Ocular biomechanics and biotransport. *Annu. Rev. Biomed. Eng*, 6:249–273, 2004.

References II

D. Evans, A. Harris, M. Garrett, H. Chung, and L. Kagemann. Glaucoma patients demonstrate faulty autoregulation of ocular blood flow during posture change. *Brit. Med. J.*, 83(7):809, 1999.

A. D. Fitt and G. Gonzalez. Fluid mechanics of the human eye: Aqueous humour flow in the anterior chamber. *Bulletin of Mathematical Biology*, 68(1):53–71, 2006.

J. Flammer, S. Orgül, and V. Costa. The impact of ocular blood flow in glaucoma. *Prog. Retin. Eye Res.*, 21(4):359–393, 2002.

J. J. Heys and V. H. Barocas. A boussinesq model of natural convection in the human eye and formation of krunberg's spindle. *Annals of Biomedical Engineering*, 30:392–401, 2002.

J. J. Heys, V. H. Barocas, and M. J. Taravella. Modeling passive mechanical interaction between aqueous humor and iris. *Transactions of the ASME*, 123:540–547, December 2001.

B. Lee, M. Litt, and G. Buchsbaum. Rheology of the vitreous body. Part I: viscoelasticity of human vitreous. *Biorheology*, 29:521–533, 1992.

J. Meskauskas, R. Repetto, and J. H. Siggers. Oscillatory motion of a viscoelastic fluid within a spherical cavity. *Journal of Fluid Mechanics*, 685:1–22, 2011. doi: 10.1017/jfm.2011.263.

J. Meskauskas, R. Repetto, and J. H. Siggers. Shape change of the vitreous chamber influences retinal detachment and reattachment processes: Is mechanical stress during eye rotations a factor? *Investigative ophthalmology & visual science*, 53(10):6271–6281, Oct. 2012. ISSN 1552-5783. doi: 10.1167/iovs.11-9390. PMID: 22899755.

References III

C. S. Nickerson, J. Park, J. A. Kornfield, and H. Karageozian. Rheological properties of the vitreous and the role of hyaluronic acid. *Journal of Biomechanics*, 41(9):1840–6, 2008. doi: 10.1016/j.jbiomech.2008.04.015.

R. Repetto. An analytical model of the dynamics of the liquefied vitreous induced by saccadic eye movements. *Meccanica*, 41:101–117, 2006. doi: 10.1007/s11012-005-0782-5.

R. Repetto, A. Stocchino, and C. Cafferata. Experimental investigation of vitreous humour motion within a human eye model. *Phys. Med. Biol.*, 50:4729–4743, 2005. doi: 10.1088/0031-9155/50/19/021.

T. Rossi, G. Querzoli, G. Pasqualitto, M. Iossa, L. Placentino, R. Repetto, A. Stocchino, and G. Ripandelli. Ultrasound imaging velocimetry of the human vitreous. *Experimental eye research*, 99(1):98–104, June 2012. ISSN 1096-0007. doi: 10.1016/j.exer.2012.03.014. PMID: 22516112.

T. W. Secomb. *Modeling and Simulation of Capsules and Biological Cells*, chapter 4. Mechanics of red blood cells and blood flow in narrow tubes. Chapman and Hall/CRC, 1 edition, May 2003. ISBN 1584883596.

I. A. Sigal, J. G. Flanagan, I. Tertinegg, and C. R. Ethier. Finite element modeling of optic nerve head biomechanicsp. *Investigative ophthalmology & visual science*, 45(12):4378–4387, December 2004.

I. A. Sigal, J. G. Flanagan, and C. R. Ethier. Factors influencing optic nerve head biomechanics. *Investigative Ophthalmology & Visual Science*, 46(11):4189–4199, November 2005.

References IV

J. H. Siggers and C. R. Ethier. Fluid mechanics of the eye. *Annual Review of Fluid Mechanics*, 44 (1):347–372, 2012. doi: 10.1146/annurev-fluid-120710-101058.

K. Swindle, P. Hamilton, and N. Ravi. In situ formation of hydrogels as vitreous substitutes: Viscoelastic comparison to porcine vitreous. *Journal of Biomedical Materials Research - Part A*, 87A(3):656–665, Dec. 2008. ISSN 1549-3296.

R. I. Tanner. *Engineering Rheology*. Oxford University Press, USA, 2 edition, May 2000. ISBN 0198564732.

T. Yamamoto and Y. Kitazawa. Vascular pathogenesis of normal-tension glaucoma: a possible pathogenetic factor, other than intraocular pressure, of glaucomatous optic neuropathy. *Prog. Retin. Eye Res.*, 17(1):127–143, 1998.

D. Yan, F. Coloma, A. Metheetrairut, G. Trope, J. Heathcote, and C. R. Ethier. Deformation of the lamina cribrosa by elevated intraocular pressure. *Brit. J. Ophthalmol.*, 78(8):643–648, 1994.